HHS Public Access

Author manuscript

Life Sci. Author manuscript; available in PMC 2024 September 15.

Published in final edited form as:

Life Sci. 2023 September 15; 329: 121970. doi:10.1016/j.lfs.2023.121970.

Theranostics in targeting fibroblast activation protein bearing cells: Progress and challenges

Sahar Rezaei[a,b], **Esmaeil Gharapapagh**[b], **Shahram Dabiri**[b], **Pedram Heidari**[c], **Ayuob Aghanejad**[a,b,*]

[a]Research Center for Pharmaceutical Nanotechnology, Tabriz University of Medical Sciences, Tabriz, Iran

[b]Department of Nuclear Medicine, Faculty of Medicine, Imam Reza General Hospital, Tabriz University of Medical Sciences, Tabriz, Iran

[c]Departments of Radiology, Massachusetts General Hospital, Boston, United States

Abstract

Cancer cells are surrounded by a complex and highly dynamic tumor microenvironment (TME). Cancer-associated fibroblasts (CAFs), a critical component of TME, contribute to cancer cell proliferation as well as metastatic spread. CAFs express a variety of biomarkers, which can be targeted for detection and therapy. Most importantly, CAFs express high levels of fibroblast activation protein (FAP) which contributes to progression of cancer, invasion, metastasis, migration, immunosuppression, and drug resistance. As a consequence, FAP is an attractive theranostic target. In this review, we discuss the latest advancement in targeting FAP in oncology using theranostic biomarkers and imaging modalities such as single-photon emission computed tomography (SPECT), positron emission tomography (PET), computed tomography (CT), fluorescence imaging, and magnetic resonance imaging (MRI).

Keywords

Fibroblast activation protein (FAP); Theranostic; Imaging; Fluorescence; PET; SPECT

1. Introduction

The tumor microenvironment (TME) is composed of cancer cells and endogenous stromal cells (such as fibroblasts and vascular cells) immune cells, and extracellular matrix (ECM) [1]. Cancer cells interact heterotypically with TME to develop tumors, evade immunity, metastasize, and become resistant to treatment [2]. The tumor mass consists of stromal cells (tumor stroma) connected by desmoplastic reactions. As critical oncological factors that determine cancer cell behavior and disease progression, ECM remodeling and TME

*Corresponding author at: Research Center for Pharmaceutical Nanotechnology, Tabriz University of Medical Sciences, Tabriz, Iran. aghanejaday@tbzmed.ac.ir (A. Aghanejad).

Declaration of competing interest

The authors declare that they have no known competing financial interests or personal relationships that could have appeared to influence the work reported in this paper.

components have recently attracted a great deal of attention [3,4]. In the TME, Fibroblasts play a crucial role in all stages of cancer metastasis and progression [5].

Cancer-associated fibroblasts (CAFs) are the most abundant fibroblasts in most solid tumors, including breast, prostate, pancreatic, and ovarian tumors [6,7]. On the whole, CAFs comprise approximately 80 % of the total fibroblast population in the TME [8]. Biochemical crosstalk between CAFs and TME plays an essential role in immunosuppression, angiogenesis, and cancer cells' metabolic reprogramming, and invasion [9,10]. CAFs facilitate tumorigenesis by secreting growth factors, chemokines, cytokines, and matrix metalloproteinases that stimulate communication between cells and remodeling of the extracellular matrix [11].

CAFs express a variety of biomarkers, making them ideal targets for theranostic purposes. Most importantly, they express a high level of fibroblast activation protein (FAP), which contributes to cancer progression and immune suppression, metastasis, invasion, and migration of cancer. FAP is a type II transmembrane serine protease with endopeptidase activity that breaks down collagen type I through proteolytic activity during matrix reorganization [12]. As part of its structure, FAP has 760 amino acids that 1–4 amino acids are found in the intracellular domain, 5–25 in the transmembrane domain and 26–760 in the extracellular domain [13]. It modulates the fibrillar organization of collagen and fibronectin and enhances tumor invasion [14]. Contrary CAFs, FAP is non-expressed in benign epithelial tumor stroma and healthy fibroblasts. Rapid and effective internalization of FAP within tumor stroma renders it an attractive biomarker in tumor stroma. FAP, even though its role in cancer prognosis remains unclear in various literature reports, can be considered a promising theranostic target [13]. As a result of targeting FAP, ECM degradation occurs, which impairs regulatory signals and stromal CAFs' supporting biological functions on tumor growth [15]. Moreover, breaking down the stroma barrier will also enhance the efficacy of other treatments, including pharmacologic, immunologic, radiation-based, or cell-based therapies [12]. Several ligands have been reported as part of the ongoing development of FAP targeting agents. Peptides, FAP inhibitors, and antibodies are the three main categories [16].

Besides the extracellular matrix, cancer tissues consist of cancer cells and surrounding stromal cells [10]. As a new index for the predictability of all-cause mortality in solid tumors, tumor-stroma ratio gives the percentage of neoplastic cells *vs.* tumor-associated stroma [17]. Although FAP expression is higher in stroma-high tumors, the stroma-high tumors also have a poor prognosis in solid epithelial tumors such as non-small cell lung cancer, colorectal cancer, hepatocellular carcinoma, breast cancer, esophageal cancer, and cervical cancer. Furthermore, short overall survival was associated with low tumor–stroma ratios (high stromal content) [18].

In FAP-expressing tumors, the radiolabeled FAP tracers can deliver image-enhancing photons and/or ionizing particles directly into the tumor stroma, allowing for nuclear imaging and/or radionuclide treatment. As an alternative to nuclear molecular imaging, FAP-based targeting radiolabeled inhibitors might offer a better way to detect tumors that have low or heterogeneous glucose metabolisms, so that nonspecific uptake could result in

a high background signal if they are located near highly glycolytic tissues [19]. Because stroma makes up a significant part of the tumor volume, radiotracers that target FAP may enhance target sensitivity and image contrast [13].

Targeted imaging of FAP could play a role in managing cancer patients [20]. In this review, we summarize the theranostic tracers for targeting FAP in cancer, with a particular focus on using these for diagnosis and therapy. Moreover, the potential benefits and challenges of using FAP-targeted ligands in oncology are discussed.

2. Targeted imaging of FAP

FAP can be broadly imaged using single-photon emission computed tomography (SPECT), positron emission tomography (PET), magnetic resonance imaging (MRI) and fluorescence imaging [21,22]. In general, molecular imaging tools include three elements: 1) a reporter molecule that produces a signal that is detectable with the help of a suitable scanner, 2) a targeting molecule that binds specifically to a molecule of interest, and 3) a linker between these two molecules [23,24].

2.1. Targeted fluorescence imaging of fibroblast activation protein in cancers

Using fluorophores with long excitation and emission wavelengths, *in vivo* fluorescence imaging can assess the pharmacokinetics and distribution of biomolecules in living tissues. Cancer can be diagnosed using these features, and tumor margins can be visualized during oncological surgery [25]. Light is scattered and attenuated in biological tissues, and incident photons are backscattering, resulting in relatively shallow penetration depths when using fluorescence imaging [26]. Near-infrared fluorophores with emission and excitation in the 650–1350 nm window are best for this since they penetrate deep into tissues and exhibit a low autofluorescence. Consequently, theranostics and drug delivery systems, diagnostic probes, and studies on disease pathogenesis are more frequently developed using fluorescence imaging in preclinical settings [27,28]. As mentioned above, overexpression of FAP by tumor-associated fibroblasts promotes tumor progression, making it a promising therapeutic and diagnostic target. Thus, conjugating the FAP ligand to the fluorescent dye offers the potential to target the tumor microenvironment with an innovative probe. Several near-infrared fluorescent dyes have been reported to target FAP (Table 1).

2.2. [^{18}F] F-labeled FAPIs for targeted imaging of FAP

Since FAP overexpress in various kinds of cancers, targeting FAP by radiolabeled FAP-inhibitors (FAPI) has impressive benefits in the diagnosis/treatment of cancers. Among radiotracers, PET radiotracers have evinced striking efficacy in targeted imaging of FAP-expressing tumors [38,39]. Due to its ability to deliver large doses over long distances, ^{18}F is a commonly used radionuclide in PET imaging.

Currently, aluminum-[^{18}F] fluoride-labeled FAPIs ([^{18}F] AlF-FAPI) have been used in several preclinical and clinical studies to develop FAP-targeting agents. To prepare [^{18}F] AlF-P-FAPI imaging probe of cancer-associated fibroblasts, Al^{18}F-chelated to pharmacophore FAP inhibitor through a polyethylene glycol (PEG) linker, which involves the NOTA chelator. Compared to [^{18}F] FAPI-42 and [^{68}Ga] Ga-FAPI-04, [^{18}F] AlF-P-FAPI

displayed greater retention and uptake of tumors. Further, [^{18}F] AlF-P-FAPI PET/CT demonstrated similar findings for primary tumors and lymph node metastases in a nasopharyngeal carcinoma patient [40].

In a study, [^{18}F] AlF-NOTA-FAPI-04 was used for PET/CT imaging of patients with advanced lung cancer, which identified the metastatic lesions more accurately than [^{18}F] FDG and facilitated tumor staging [41]. In another study, PET/CT imaging using [^{18}F] AlF-NOTA-FAPI-04 (^{18}F-FAPI) in 20 patients to assess physiological distributions and benign lesion incidental uptake revealed that various cancer types are associated with incidental benign lesion tracer uptake, so benign lesion ^{18}F-FAPI uptake can lower ^{18}F-FAPI PET/CT specificity [42].

Recently, the role of [^{18}F] F-FAPI PET/CT on the staging of primary lung adenocarcinoma (LAD) was examined on thirty-four LAD-bearing patients, [^{18}F] F-FAPI has an excellent detection rate for primary LAD and clear tumor delineations. Moreover, this radiotracer indicated more lesions than [^{18}F] F-FDG, especially in lymph nodes, the brain, and the pleura. Results revealed that [^{18}F] F-FAPI was more reliable for primary LAD staging than [^{18}F] F-FDG, but brain MRI is capable of identifying smaller and more numerous lesions than [^{18}F] F-FAPI PET/CT [43].

Depending on the type of tumor and its interaction with the stroma, monospecific tracers will not be efficient for tumor diagnosis/treatment. A heterodimer dual targeting of specific membrane antigen (SMA) and FAP may improve tumor diagnosis or treatment in tumors that overexpress SMA and upregulate FAP in the tumor stroma [44,45]. In order to noninvasively visualize tumors with a combination of receptor expression patterns, Hu and colleagues developed ^{18}F-labeled bispecific heterodimer radiotracers that target both PSMA and FAP. Fig. 1A, B shows that the tumor was visible shortly following injection (15 min), and the contrast gradually improved during the PET scan wore on with both heterodimeric tracers. As well as superior retention and quick uptake in tumors, ^{18}F-labeled PSMA-FAP heterodimeric radiotracers also demonstrated fast clearance through the kidney of nontarget tissues (Fig. 1C, D). For both of them, muscle, heart, brain, lung and liver function were low [46].

Compared with FDG, FAPI is more sensitive in areas with greater levels of glucose metabolism, does not require fasting, and allows for rapid image acquisition. Furthermore, FDG's high physiological uptake does not mask metastases. FAP targeting tracers with ^{18}F labels are, therefore, in high demand. As the FAP tracer for PET imaging, [^{18}F] AlF-P-FAPI has higher specificity than [^{18}F] FDG, irrespective of blood sugar or physical activity.

Hepatobiliary physiological uptake of ^{18}F-labeled FAPI interferes with the detection of lesions located in or adjacent to the hepatobiliary system [47]. However, the FAPI radiotracers could not suitable for PET imaging of cancers in hepatobiliary systems. Recently [^{18}F]FAPT, a novel tracer with PEG2-glycopeptide modification of FAPI pharmacophore, was developed to reduce hepatobiliary physiological uptake of [^{18}F]-labeled FAPI tracers. High specificity for FAP-targeting was observed in [^{18}F] FAPT, the radioactivity was extremely stable both *in vitro* and *in vivo* within all observed times. It is

important to note that [^{18}F]FAPT has a drawback, due to significant physiological uptake in salivary glands, thyroid, and pancreas [48].

2.3. [^{68}Ga]Ga-labeled FAPIs for targeted imaging of FAP

In spite of promising results in tumor diagnosis, the retention time of tumors treated with peptide-targeted radionuclides is relatively short when using FAP-targeted molecular imaging agents. In this regard, Ga-FAPI-[^{68}Ga] demonstrated excellent biodistribution and an impressive tumor-to-background ratio [15,49,50]. In terms of publications and active trials, [^{68}Ga] Ga-FAPI imaging has seen a recent surge in interest.

In order to optimize the pharmacokinetics, the performance of FAPI dimer ^{68}Ga-DOTA-2P $(FAPI)_2$ was compared with that of ^{68}Ga-FAPI-46 in human xenografts and three cancer patients. In addition to being an imaging agent capable of effectively detecting malignant tumors expressing FAP, ^{68}Ga-DOTA-2P $(FAPI)_2$ has improved uptake and retention properties for tumors over ^{68}Ga-FAPI-46 (Fig. 2) [42].

Moreover, a study conducted recently found that a new CAF-targeting tracer [^{68}Ga]Ga DATA^{5m}.squaric acid (SA).FAPI has also allowed visualization of different carcinomas and metastases associated with cancerous fibroblasts (prostate cancer, parotid tumors, NSCLC, liposarcoma, and pancreatic cancer), but there was minimal uptake in the bone, intestine, liver, lungs and brain [51].

PSMA expression heterogeneity in cancer of the prostate makes PSMA ligand PET ineffective in patients with low or negative PSMA expression. By targeting both PSMA and fibroblast activation proteins at once, prostate cancer diagnostic accuracy may be improved. For prostate cancers with low or negative PSMA expression, a PSMA-FAPI heterodimer was synthesized to create a PSMA/FAP dual-target heterodimer. [^{68}Ga] Ga-PSMA-FAPI's performance in PET/CT diagnostics of tumor-bearing mice was evaluated compared to [^{68}Ga] Ga-FAPI-04 and [^{68}Ga] Ga-PSMA-11.From the results, it was evident that PSMA-FAPI heterodimer PET/CT not only targets PSMA-positive prostate cancer but also improves the diagnosis of PSMA-negative prostate cancer [52].

Integrin αvβ3 is a promising target for imaging and treating tumors due to its significant ability to regulate tumor growth, invasion, angiogenesis, and tumor metastasis [53]. Although, radiolabeled cyclic arginine-glycine-aspartate (RGD) peptides with integrin αvβ3 specificity can be used to evaluate angiogenesis and tumor growth [54,55]. RGD-based radiotracers, however, have only shown moderate tumor uptake [56]. Targeting both FAP and αvβ3 by developing bi-specific heterodimeric radiotracers indicated that tumor uptake and retention can be significantly improved by [^{68}Ga] Ga-FAPI-RGD in both animal and human models. Furthermore, high TBRs of [^{68}Ga] Ga-FAPI-RGD over time led to higher diagnostic performance and more effective therapy [57]. PET/CT imaging with ^{68}Ga-FAPI-RGD in various types of cancer showed that the activity of this radiotracer is significantly reduced in normal organs (including the thyroid, pancreas, and salivary glands, whereas tumor lesions showed enhanced uptake from 0.5 to 3 h after injection, leading to optimal lesion contrast in delayed scans [58].

In cancer patients, FAPI PET uptake is highly correlated with FAP expression, making FAPI PET an effective biomarker for FAP-targeted therapeutic approaches. In this regard, immunohistochemistry in 141 patients assessed FAP expression across various types of cancer using a pan-cancer human tissue microarray and showed that ^{68}Ga-FAPi-46 PET biodistribution in cancerous and non-cancerous tissues adjacent to tumors was significantly correlated with FAP expression. It appeared that stromal areas nearby and within malignant epithelial compartments (peritumoral) had the highest staining intensity [59].

[^{68}Ga]GA-FAPI-46 was found to detect nodes and hematomas in urothelial carcinoma lesions before systemic treatment using Unterrainer et al. Among 64 detected tumor sites using PET or CT, lymph node metastases and the primary site had the highest uptake intensity. Interestingly, CT imaging revealed lesions with suspected metastatic sides, but no FAPI expression; histopathology ruled out malignancies [60].

Retrospective analysis of liver malignancies found the [^{68}Ga] Ga-FAPI-46 PET/CT along with liver-specific PET/MRI to be 100 % sensitive for detecting intrahepatic lesions. By comparison, [^{18}F] FDG PET/CT showed only 58 % sensitivity. Intrahepatic tumors with [^{68}Ga] Ga-FAPI had greater SUV_{max} and target-to-background ratios than those with [^{18}F] FDG, suggesting that primary intrahepatic tumors can be evaluated noninvasively. Further, [^{68}Ga] Ga-FAPI-46 PET/CT revealed 100 % positivity for regional node metastases as compared to 58 % for [^{18}F] FDG PET/CT [61].

^{68}Ga-DOTA-FAPI-04 shows high sensitivity for primary carcinomas and metastatic disease [44–47], a greater contrast between tumor and background [48, 49], and a lower gastrointestinal uptake. PET/MR with ^{68}Ga-DOTA-FAPI-04 is more accurate than ^{18}F-FDG PET/CT in detecting gastric cancer metastases and primary tumors, as well as lymph nodes in the peritoneum and abdomen (Fig. 3) [43].

Compared with [^{18}F] FDG PET/CT imaging in the early pancreatic adenocarcinoma detection using an orthotopic xenograft model from patients, [^{68}Ga] FAPI-04 in various organs was remarkably high. Moreover, the effectiveness of the early detection of the [^{68}Ga] FAPI-04 probe was also confirmed using B-mode ultrasound and near-infrared fluorescence imaging (NIRF). Thus, an improved surgical plan, staging, and early diagnosis along with treatment response monitoring may be possible with this radiotracer [62]. A semi-quantitative analysis of [^{68}Ga] Ga-FAPI-04 tumor uptake in nine patients with pancreatic cancer was also performed using the tumor-to-blood ratio (TBR). An effective index for tumors with high FAP levels in theranostics was developed, demonstrating a statistically significant correlation between TBR_{mean} and total distribution volume in theranostics. Interestingly TBR_{mean} indicated a higher FAP receptor density than SUV_{mean} and SUV_{max} [63]. In a retrospective study on patients suffering from pancreatic cancer, the [^{68}Ga] Ga-FAPI-04 accumulation was strongly related to the *ex vivo* FAP expression and aggressive pathology. Moreover, [^{68}Ga]Ga-FAPI-04 showed potential for cancer prognosis [64].

Due to ^{18}F-FDG accumulation in acute inflammatory lesions, high FDG uptake occurs in the intestine nonspecifically. Consequently, It is possible to observe high FDG uptake in various colon and rectum diseases, such as tumors, polyps, Crohn’s disease, or colitis [65,66].

To solve this challenge, Shangguan et al. suggested substituting ^{68}Ga-FAPI-04 PET for ^{18}F-FDG PET to resolve the challenge of distinguishing inflammatory diseases from malignant tumors in colorectal cancer patients [67]. It was also found that the FAPI-04 signal was low or nonexistent in inflammatory lesions in addition, rat CRC tumors induced by AOM/DSS absorb ^{68}Ga-FAPI-04 PET well and create a strong contrast between tumor and background. Accordingly, ^{68}Ga-FAPI-04 PET specificity was much higher than 18F-FDG PET in colorectal cancer patients. The low gastrointestinal uptake and tumor-to-background activity of ^{68}Ga-FAPI-04 PET/CT also improve colorectal cancer staging. Furthermore, ^{68}Ga-FAPI-04 PET/CT is more effective at finding distant metastases and lymph nodes than ^{18}F-FDG PET/CT [57].

[^{68}Ga]Ga-DOTA-FAPI-04 imaging agent can detect multiple tumor types and inflammations, especially non-oncological lesions and solid tumors [68,69]. It has recently been shown that [^{68}Ga] Ga-DOTA-FAPI-04 PET/CT is more effective at detecting primary and metastatic tumors than [^{18}F] FDG PET/CT [63]. There are extremely high SUV_{max} levels observed in pancreatic, liver, and stomach duct adenocarcinomas compared to [^{18}F] FDG PET/CT. Additionally, [^{68}Ga]Ga-DOTA-FAPI-04 PET/CT was evaluated in 29 colorectal cancer patients who had recently been diagnosed or had recently relapsed. Compared to [^{18}F]FDG PET/CT, [^{68}Ga]Ga-DOTA-FAPI-04 is significantly more sensitive and specific in the detection of peritoneal metastases, lymph nodes, and primary malignancies [40]. In light of the fact that [^{68}Ga]Ga-DOTA-FAPI-04 may yield better clinical staging results than 2-[^{18}F] FDG PET/CT, its application is gaining attention. This approach investigated [^{68}Ga] Ga-DOTA-FAPI-04 PET/CT as an imaging biomarker for tumor staging in 134 non-small cell lung cancer (NSCLC) patients. There was an increased staging accuracy in [^{68}Ga] Ga-DOTA-FAPI-04 compared to 2-[^{18}F] FD [43/52 (82.7 %) *versus* 27/52 (51.9 %), P = 0.001] [70].

In order to assess the effectiveness of the newly developed FAP-targeted radiotracer, 64 cancer patients underwent ^{68}Ga-FAP-2286 PET/CT for diagnosis and recurrence detection. Compared to ^{18}F-(FDG), ^{68}Ga-FAP-2286 offered better image contrast and lesion detectability than ^{18}F-(FDG) in primary tumors, distant metastases, and lymph node metastases. Furthermore, the tumor uptake and lesion detectability rate were the same in ^{68}Ga-FAP-2286 and ^{68}Ga-FAPI-46 [71]. In muscles, salivary glands, thyroid, and pancreas, ^{68}Ga-FAP-2286 showed a lower physiologic uptake than ^{68}Ga-FAPI-46. However, the cyclopeptide structure of FAP-2286 may alter the *in vivo* pharmacokinetics due to greater uptake in kidneys, livers, and hearts than that of ^{68}Ga-FAPI-46. Furthermore, Lymph node and visceral metastasis imaging with ^{68}Ga-FAP-2286 showed higher uptake and TBR compared to ^{18}F-FDG for detecting metastases, especially those in the liver, bones, and peritoneum. Therefore, it has been observed that FAP-2286 is more likely to increase FAP binding affinity, accumulate tumors better, and retain tumors longer than other FAPI variants. In addition, ^{68}Ga-FAP-2286 PET/CT can be used to diagnose cancers for which ^{18}F-FDG PET/CT is ineffective [72].

Clinical target volumes (CTV) are usually large for patients with adenoid cystic carcinoma (AC), pancreatic ductal adenocarcinoma (PDAC), and biliary tract carcinoma (BTC)·In a study involving 41 patients with AC, PDAC, and BTC, [^{68}Ga] FAPI-PET/CT was used to

assess pre- and post-treatment response and define radiotherapy target volumes. There is some evidence that [^{68}Ga] FAPI-based planning can cover both plain macroscopic gross tumor volume as well as [^{18}F] FDG volume, compared to [^{18}F] FDG-based planning, which cannot fully cover [^{68}Ga] FAPI volume. Hence, [^{68}Ga] FAPI offers an effective imaging method for this particular patient population, enabling better planning of radiotherapy and assessing treatment response [73].

In recent years, FAPI-PET/CT has demonstrated that it is a very useful tool in imaging non-malignant conditions, especially those related to inflammation [74,75]. A retrospective analysis of ^{68}Ga-FAPI-02, FAPI-46, and FAPI-74 for malignant, inflammatory, and degenerative lesions revealed that accumulation was more prominent for all three tracer variants in both malignant and inflammatory/reactive lesions than in degenerative lesions [76]. Overall, FAPI PET/CT applications in inflammation have been relatively limited compared with those in oncology. However, there is not enough data available to translate this research into clinical practice, raising the possibility of additional research into FAPI PET in inflammatory diseases. FAPI PET/CT may be used in clinical practice for selected inflammatory conditions in the coming years due to the increased availability of FAPI radiotracers worldwide.

Within a single session, clinical evaluations using dual-tracer [^{18}F] FDG/[^{68}Ga]Ga-FAPI-46 PET/CT have demonstrated success in cancer diagnosis using this technique. Compared to [^{18}F]-FDG PET/CT alone, PET/CT with dual-tracer technology was more sensitive and had higher target-to-background ratios [77].

Although FAP-targeting tracers have proven promising, they have some pitfalls that influence their applications. For instance, uptake of [^{68}Ga] Ga-FAPI-04 and [^{68}Ga]Ga-FAPI-46 by degenerative lesions in joints, vertebral bones, muscles, scars, and head and neck has been observed [78]. Moreover, nonspecific and off-target uptake of quinoline-based FAP tracers causes challenges to identify FAP-positive tumor lesions [79,80]. However, developing pyridine-based tracers for targeting FAP would overcome these limitations [81].

2.4. Targeted SPECT imaging of FAP

Targeting CAFs with radiopharmaceuticals has gained an increasingly popular strategy for cancer diagnosis and treatment. As a result of their lower cost and more widespread availability, nuclear medicine studies using SPECT still account for >70 % of the total. Radiopharmaceuticals labeled with ^{99m}Tc are increasingly needed in oncology since ^{99m}Tc is the most popular radionuclide used in SPECT imaging. The design and synthesis of Tc-99 m-((*R*)-1-((6-hydrazinylnicotinoyl)-D-alanyl) pyrrolidine-2-yl) boronic acid ([^{99m}Tc] Tc-FAPI) was recently demonstrated as a suitable radioligand for SPECT tumor microenvironment imaging based on ^{99m}Tc-HYNIC-D-alanine-boroPro, a novel FAP inhibitor radioligand. According to the results of the analyses, the radiotracer was highly stable in human serum (>95 % after 24 h), specifically recognized FAP, and was uptaken highly (7.15 % ID/g after 30 min) by tumors, and showed rapid elimination by the kidneys. To establish ^{99m}Tc-FAPI's specificity and sensitivity for tumor imaging, more clinical and dosimetric studies are warranted [82].

Moreover, an ideal chelator for radiolabeling with ^{99m}Tc, HYNIC, contains two nitrogen atoms from the hydrazine group and offers high radiolabeling yield, stability, and hydrophilicity [83]. Recent studies revealed that the ^{99m}Tc-HYNIC-FAPI is more sensitive to FAP-expressing tumors [84]. Due to the popularity of SPECT/CT over PET/CT and recent advances in quantification and resolution, ^{99m}Tc-HYNIC-FAPI has proven to be a promising small molecular probe for SPECT/CT tumor imaging.

As a result of the clinical evaluation of lyophilized formulations prepared under GMP conditions, [^{99m}Tc] Tc-FAPI SPECT imaging provides valuable prognostic information, especially for solid tumors such as breast cancer. Six cancerous entities were evaluated for tumor stroma imaging with the newly developed radioligand, and the tumor stroma's heterogeneity was analyzed. A total of four high-grade gliomas were found to be positive with [^{99m}Tc] Tc-FAPI imaging. Furthermore, [^{99m}Tc] Tc-FAPI uptake (Bq/cm3) in primary tumors was correlated with molecular subtypes, with HER2+ and HER2-enriched Luminal B exhibiting the highest uptake values. As a consequence of rapid blood activity removal and renal clearance, this study's results demonstrated good biodistribution and kinetics and high and reliable uptake of [^{99m}Tc] Tc-FAPI in primary tumor lesions as well as lymph nodes of breast, cervical, and lung cancer patients. Results showed potential differences in prognostic evaluations between different types of cancer, along with superior diagnostic evaluations when compared with peritoneal carcinomatosis. In summary, the analyses confirmed that [^{99m}Tc] Tc-FAPI is not intended to replace metabolic, molecular imaging but acts as a complement to passable prognostics [85].

Another clinical trial evaluated the dosimetric and kinetic characteristics of [^{99m}Tc] Tc-FAPI in six healthy volunteers and raditracer uptake from various solid tumors in three cancer patients. According to the results, breast, cervical, and lung cancer patients had sufficient concentrations of the [^{99m}Tc] Tc-FAPI radioligand in their lymph nodes and primary tumors. Consequently, [^{99m}Tc] Tc-FAPI SPECT/CT had an excellent correlation with [^{18}F] FDG PET/CT for the detection of primary and metastatic tumors (Fig. 4). Finally, dosimetry results indicate that imaging with [99mTc] Tc-FAPI can potentially be used for measuring tumor microenvironment FAP expression based on tumor-to-background ratios (T/B) [86].

In a recent study, researchers provide a potential new tool for imaging malignant tumors. Most malignant epithelial neoplasms express more FAP than CAFs, which is the basis for this proposal. The probe was designed for ^{99m}Tc radiolabeling using the chelator 6-hydroxyzinylnicotinic acid (HYNIC). *In vitro* binding to MCF-7 human breast cells was achieved using ^{99m}Tc-HYNIC-FAPI, as well as superior radiochemical purity and stability. Additionally, the probe inhibited tumor cell migration and showed binding properties. Findings like these may lead to a deeper understanding of disease progression and a more accurate diagnosis, potentially enabling a more accurate tumor imaging. Recently, newly developed FAP-ligand (FL) [^{99m}Tc] Tc-FL-L3 has been introduced for triple-negative breast cancer imaging. Accumulation of tracer in solid tumors was detected *via* SPECT analysis. Upon coinjection of cold FL excess, tumor uptake was prevented, suggesting the radiotracer was retained by FAP. It was also shown that FL-L3-^{99m}Tc could localize malignant lesions in whole-body images. Accordingly, monitoring CAF-directed therapies could also be performed with SPECT or PET imaging agents targeting FAP [37]. Moreover, the

hydrophilic ^{99m}Tc-labeled complexes such as [^{99m}Tc]Tc-L1, [^{99m}Tc]Tc-L2, and [^{99m}Tc]Tc-DP-FAPI that obtained from FAP ligands (L1,L2, DP) indicated higher sensitivity to FAP-expressing tumors than the other hydrophilic complexes. They showed greater tumor uptake and higher tumor-to-nontarget ratios [87,88].

The performance of [^{99m}Tc] Tc-sb03055 against [^{68}Ga] Ga-FAPI-04 was assessed in male NRG mice bearing HEK293T:hFAP tumor xenografts in order to develop, optimize, and evaluate ^{99m}Tc-based FAP inhibitors for SPECT imaging. [^{68}Ga] Ga-FAPI-04 demonstrated superior uptake and retention in tumors to [^{99m}Tc] Tc-sb03055. Likewise, because of its high lipophilicity, [^{99m}Tc] Tc-sb03055 was retained in most organs, resulting in low-contrast images. As a result, hydrophilic fragments must be synthesized to incorporate into SB03055 to produce inhibitors with lower lipophilicity. In addition to increasing tumor uptake and image contrast, this approach reduces the retention of blood and organs as well [89].

Researchers designed and evaluated FAPI variants containing ^{99m}Tc-binding chelators *in vitro* and *in vivo*. During the formation of Tc (I) tricarbonyl complexes, quinolone-based FAPIs were presented attached to a polydentate chelator. Hydrophilic amino acids were added to the chelator to improve the pharmacokinetics of the compounds with different linker lengths. FAPI tracers with ^{99m}Tc labels displayed high binding ability, excellent affinity, and strong tumor uptake. Since ^{99m}Tc-FAPI-34 achieved the highest contrast by rapidly absorbing tumor tissue and clearing it from the rest of the body, it was chosen for SPECT imaging in patients with metastatic pancreatic and ovarian cancer following treatment with ^{90}Y-FAPI-46. Despite its limitations, this first-in-human study offered promising results (Fig. 5) [90].

According to a recent study, [^{99m}Tc][Tc-(CN-PEG$_4$-FAPI)$_6$]$^+$ and [^{99m}Tc][Tc-(CN-C5-FAPI)$_6$]$^+$ were obtained by synthesizing two isocyanide-containing FAP inhibitors (CN-C5-FAPI and CN-PEG4-FAPI). Furthermore, a greater tumor uptake and tumor-to-nontarget ratio have been observed with [^{99m}Tc][Tc-(CN-PEG$_4$-FAPI)$_6$]$^+$ than with [^{99m}Tc][Tc-(CN-C5-FAPI)$_6$]. It follows that [^{99m}Tc][Tc-(CN-PEG$_4$-FAPI)$_6$]$^+$ would be an interesting target for tumor imaging using FAP as well [91].

3. Therapeutics for targeting FAP

A lack of tumor retention and rapid clearance of fibroblast activation proteins in cancer therapy have hampered their clinical translation. To meet this challenge and overcome this limitation, Wen et al. developed a series of Evans blue (EB) modified FAP-targeted radiotracers that included a truncated albumin binder. As a result of synthesizing several radiopharmaceuticals related to EB-modified fibroblast activation protein inhibitors (FAPI-02), they found that the ^{177}Lu-EB-FAPI-B1 demonstrated reduced normal tissue uptake and significantly enhanced tumor retention, as well as increased binding affinity and specificity of targeting *in vitro*. A significant reduction in tumor growth was observed with [^{177}Lu] Lu-EB-FAPI-B1 in the U87MG tumor model without adverse side effects, suggesting potential clinical applications for this compound (Fig. 6) [92]. Another study found that new radiopharmaceuticals based on FAPI for FAP-targeted radiotherapy were superior to existing alternatives. A truncated Evans blue moiety (TEFAPI-07) and 4-(*p*-

iodophenyl)butyric acid moiety (TEFAPI-06) were selected as FAPI-04 binders. In the process of synthesizing TEFAPI-07 and TEFAPI-06, they were labeled with ^{177}Lu. In PDX animal models, ^{177}Lu-TEFAPI-06 and ^{177}Lu-TEFAPI-07 were assessed for SPECT imaging, biodistribution studies, and therapeutic efficacy. Not only did ^{177}Lu-TEFAPI-06 and ^{177}Lu-TEFAPI-07 improve tumor retention and uptake compared to ^{177}Lu-FAPI-04, but they also effectively inhibited PDX tumor growth while showing virtually no side effects. To develop FAP-targeted radiotheranostics, Evans blue modification followed by albumin binding and labeling with ^{177}Lu is a critically important strategy for modifying the pharmacokinetics and pharmacodynamics of relatively lipophilic FAPI derivatives [57]. According to Wen et al., biodistribution analyses and SPECT imaging of [^{177}Lu] Lu-DOTA-EB-FAPI confirmed enhanced tumor accumulation and retention in U87MG and HepG2-FAP xenograft models. Moreover, [^{177}Lu] Lu-DOTA-EB-FAPI at different doses significantly inhibited tumor growth. By conjugating albumin binders with FAPI-based radiopharmaceuticals, FAPI-based radiopharmaceuticals can become more effective at enhancing tumor uptake, which may let them transform their diagnostic capabilities into therapeutic properties [93].

An albumin-binding moiety was conjugated to FAPI molecules to overcome the challenge of insufficient uptake and retention by tumor cells. FAPI radiopharmaceuticals bound to albumin were prepared by conjugating palmitic acid (C16) and lauric acid (C12) to FAPI-04, which was then radiolabeled with ^{177}Lu. There was a greater tumor uptake of [^{177}Lu] Lu-FAPI-C16 than [^{177}Lu] Lu-FAPI-C12, and both were greater than [^{177}Lu] Lu-FAPI-04. Moreover, Survival was 28 days for the [^{177}Lu] Lu-FAPI-C16 treated group compared to 10 days for the [^{177}Lu] Lu-FAPI-04 treated group. It has been shown that using albumin binders such as Evans blue and 4-(*p*-iodophenyl) butyric acid to prolong the blood circulation of radiopharmaceuticals or small molecules can enhance the effectiveness of anticancer drugs by improving therapeutic dose delivery [94].

To optimize pharmacokinetics, Zhao et al. designed FAPI dimer (denoted DOTA-2P $(FAPI)_2$). With the aid of FAPI-46, DOTA-2P $(FAPI)_2$ was synthesized and radiolabeled with ^{177}Lu. It was observed that ^{177}Lu-DOTA-2P $(FAPI)_2$ had more uptake on cell-derived xenografts (CDXs) and patient-derived xenografts (PDXs) after SPECT imaging in both cases. Biodistribution analysis revealed that [^{177}Lu] Lu-DOTA-2P $(FAPI)_2$ had greater efficacy at all time points than [^{177}Lu] Lu-FAPI-46 in CDXs and PDXs. A superior tumor growth inhibition was also demonstrated by [^{177}Lu] Lu-DOTA-2P $(FAPI)_2$ without causing any systemic side effects. Thus, ^{177}Lu-DOTA-2P $(FAPI)_2$ can be an effective and safe treatment for malignant tumors expressing FAP [95].

By providing an additional coordination site, bifunctional DOTA, and DOTAGA chelators can complex ^{177}Lu and are effective in theranostic use due to their ability to accumulate tumor material and longer tumor retention time. However, compound residence times have been a challenge for therapeutic applications. Currently, [^{177}Lu]Lu-DOTAGA. $(SA.FAPi)_2$ and [^{177}Lu]Lu-DOTA.SA.FAPi have been introduced and compared across a wide range of cancer types in terms of dosimetry, pharmacokinetics and biodistribution. [^{177}Lu]Lu-DOTAGA.$(SA.FAPi)_2$ homodimer displayed substantially better tumor retention than its monomer counterpart, although colon and kidney uptakes were greater than the first; however, each uptake was well tolerated. As a result, [^{177}Lu]Lu-DOTAGA.$(SA.FAPi)_2$

displayed accelerated internalization, increased affinity, faster clearance of non-target organs and prolonged tumor retention, opening up new therapeutic opportunities for patients with advanced cancers [96].

Two radiotracers, FAP-2286 and FAPI-46, target FAP through different mechanisms: the former uses a peptide macrocycle, whereas the latter uses a quinoline-based molecule. The imaging and therapeutic effects of FAP-2286 are currently being investigated in patients. During the preclinical study, FAP-2286's efficacy, selectivity, and potency were demonstrated, along with its strong affinity for recombinant FAP and FAP expressed on fibroblast surfaces, as well as its rapid and persistent uptake in tumors with FAP, accompanied by little uptake in healthy tissues. Besides exhibiting potent and selective FAP binding properties, FAP-2286 demonstrated substantial therapeutic efficacy and powerful tumor-targeting properties. It is, therefore possible to develop ^{177}Lu-FAP-2286 for treating and ^{68}Ga-FAP-2286 for imaging FAP-positive tumors in clinical trials (Fig. 7) [97].

^{131}I-labeled FAPI analogs were synthesized and evaluated for cancer theranostics in a recent study. As a result of the ^{131}I-FAPI-04 and ^{131}I-FAPI-02's and high lipophilicity, they are mainly excreted through the kidneys and the hepatobiliary tract. The tumor-to-organ ratio was also greater with ^{131}I-FAPI-04, as well as a prolonged dwell time and increasing accumulation. In addition to suppressing the growth of tumors in U87MG xenograft mice, ^{131}I-FAPI-04 treatment also had no adverse effects [98].

FAP inhibitors for breast cancer may benefit patients' outcomes since they slow tumor growth [99]. Loktev et al. used an inhibitor that specifically targets FAP to develop radiopharmaceuticals using small molecules. It was demonstrated *in vitro* that [^{125}I] I-FAPI-01 bound highly to FAP-expressing cells and that the tracer was rapidly internalized by the cells. After the extended incubation period, enzymatic deiodination decreased the intracellular accumulation of [^{125}I] I-FAPI-01. Theranostic tracers based on FAPI-02 were therefore chelated with DOTA or radiolabelled with ^{177}Lu or 68Ga to enhance tracer stability. There was a strong binding affinity and high uptake of [^{177}Lu] Lu-FAPI-02 *in vitro*. Additionally, [^{177}Lu] Lu-FAPI-02 retained and uptaken into cells more than [^{125}I] I-FAPI-01 [100] FAPI derivatives (03–15) were recently compared in terms of their stability, binding, and biokinetics properties. FAPI-04 was the most promising derivative from the batch of products tested for potential use as a theranostic tracer. SPECT-based theranostic analysis of [^{9}Y]-FAPI-04 confirmed the presence of metastasis tracer accumulation. In one case, [^{90}Y]-FAPI-04 was administered to a breast cancer patient who suffered from metastatic disease (2.95 GBq; 24 nmol/GBq). Injecting FAPI-04 intravenously after labeling it with a ^{90}Y-chloride solution was done using a sterile filter system that is low protein-binding. A significant reduction in pain medication intake was observed with [^{90}Y]-FAPI-04 treatment without causing any side effects [101].

An assessment of the potential for a bivalent FAP ligand (ND-bisFAP) for PET imaging and endo radiotherapy in tumor-bearing mice revealed that not only did [^{177}Lu]Lu-ND-bisFAPI and [^{18}F]AlF-ND-bisFAPI significantly increase tumor retention and uptake over existing radioligands [^{177}Lu]Lu-FAPI-04 and [^{18}F]AlF-FAPI-42 at various time points, but they also delivered four times as much radiation to tumors [102]. A new anti-Fibroblast

activation protein-α recombinant antibody (anti-FAPα rAbs) radiolabeled with ^{89}Zr and ^{177}Lu was evaluated on HT1080 tumor-bearing mice. There was a high efficacy of ^{89}Zr/177Lu-AMS002-1-Fc in inhibiting tumor growth without significant weight loss and higher tumor uptake, making it a suitable radiopharmaceutical for theranostic applications [103].

Alpha therapy targeting FAP is another treatment option for cancer, in addition to beta therapy. Finding the most optimal combination of radionuclide decay and fast FAP kinetics is crucial, combined with therapies targeting tumor cells to optimize the treatment. Thus alpha therapy assessment using [^{225}Ac] FAPI-04 was conducted by Watabe et al. for patients with pancreatic cancer expressing FAP. By emitting alpha particles from CAFs in the stroma, [^{225}Ac] FAPI-04 irradiated tumor cells. Tumor growth in human pancreatic cancer xenograft mice was significantly suppressed by [^{225}Ac] FAPI-04 injection without substantially affecting their body weight [104]. Because beta particles have a broad range in tissue, beta irradiation will likely reach tumor cells more homogeneously than alpha irradiation. Yuwei et al. used FAPI-46 labeled with ^{177}Lu, a beta emitter, to compare its therapeutic effects in pancreatic cancer xenografts expressing FAP with FAPI-46 labeled with ^{225}Ac, an alpha emitter. Three hours after administration of [^{177} Lu] and [^{225}Ac] FAPI-46, kidney clearance and tumor accumulation were rapid. Furthermore, [^{225}Ac] FAPI-46 and [^{177}Lu] FAPI-46 presented tumorsuppressing properties, leading to slight weight loss. The duration of action of [^{177}Lu] FAPI-46 was much longer than that of [^{225}Ac] FAPI-46, despite the relatively slow treatment effects [43].

Glioma is a common intracranial tumor without suitable treatment. *In vitro* and *in vivo* assessing ^{211}At-labeled FAPI's therapeutic action against gliomas was conducted to address this challenge. It was found that ^{211}At-FAPI-04 was highly stable *in vitro* and could significantly reduce the viability of FAP-positive U87MG cells, arrest the cell cycle, and suppress their proliferation. It also extended median survival and inhibited tumor growth in U87MG xenografts within a dose-dependent manner without adverse effects on normal tissues. As a result of treatment with ^{211}At-FAPI-04, apoptosis and reduced proliferation were also observed [102]. Though FAPI radiotracers offer outperforming and decent image contrast in different types of cancers, in comparison with [^{18}F]FDG [105], their tumor accumulation ratios are not sufficient for targeted radionuclide therapy. Moreover, the noteworthy clearance of FAPI radiotracers from tumor sites could further diminish their therapeutic effects. To overcome these issues, albumin-binding moieties that conjugated with radiotracers could prolong their blood circulation and improve the diagnostic and therapeutic efficacy of FAPI radiotracers [106]. Table 2 summarizes the selected FAPI radiotracers used for cancer therapy.

4. New series of FAP compounds

Modern imaging methods like CT and MRI are critical to the early detection of pancreatic ductal adenocarcinoma, which carries a poor prognosis. Although PET using ^{68}Ga-labeled FAPI effectively detects pancreatic ductal adenocarcinoma, early/small lesions may be missed because of their short half-life ($t^{1/2}$ = 67.7 min) and high positron energy (β^{+}_{mean} = 829.5 keV). Based on a recent study, ^{43}Sc-FAPI provided images with enhanced resolution in a murine model with fewer artifacts and enhanced ability to detect smaller lesions owing

to its long half-life ($t_{1/2}$ = 3.891 h) and lower positron energy (β^{+}_{mean} = 476 keV) (Fig. 8) [110].

A newly developed albumin-binding FAP ligand (denoted as FSDD0I) preloaded with ^{68}Ga, and ^{177}Lu was used by Meng et al. to improve tumor retention and uptake with most FAP-based radioligands. Following PET imaging of xenografts derived from human hepatocellular carcinoma patients, ^{68}Ga-FSDD$_0$I induces longer blood retention in animal models. Additionally, ^{177}Lu -FSDD0I has been shown to have significant tumor retention properties after SPECT imaging [111]. By developing ^{11}C-FAPIs, an innovative approach to PET imaging of diseases related to FAP, including cancer, arthritis, pulmonary fibrosis, or heart diseases, has been developed. Researchers concluded that ^{11}C-labeled FAPI-01 and ^{11}C-FAPI-02 could be used in the clinic because they increased tumor uptake and retained tumors longer than conventional FAPIs, suggesting that ^{11}C-labeled FAPI treatment could be used in the clinic and benefit from its physical imaging and short half-life. Interestingly, ^{11}C-labeled tracers can pass through the blood-brain barrier more easily and image the brain glioma more quickly than [^{68}Ga] Ga-DOTA-FAPI-04 in U87MG tumor xenografts [112]. Additionally, an optimized linker was developed to create ^{64}Cu-labeled compounds targeting FAP and PSMA, potentially allowing them to treat and image various cancers. According to *in vivo* imaging results, ^{64}Cu-FP-L1 was targeted for FAP and PSMA with high specificity and accumulated in tumors successfully [113].

A remarkable discovery in imaging and a promising treatment opportunity has been made with the discovery of OncoFAP, a PET imaging ligand with ultra-high affinity for malignant solid tumors. This ligand inspired the development of a new series of [^{18}F]AlF-OncoFAP-NOTA, [^{177}Lu] Lu-OncoFAP, and [^{68}Ga] Ga-OncoFAP. As a result of OncoFAP-based theranostics agents' increased uptake within cancerous lesions and low accumulation within normal tissues, they can image and treat patients with solid tumors [114]. OncoFAP is highly efficient at delivering ^{177}Lu and cytotoxic drugs. It has a half-life of around 6 h in tumors [115]. Therefore, a higher inhibition potency of FAP is required to prolong residence time at the tumor site, increasing radiation exposure and therapeutic effectiveness [116]. Researchers recently provided a novel and highly effective FAP ligand so-called OncoFAP-11. Results showed the affinity-matured [^{177}Lu] Lu-OncoFAP-11 and its bivalent derivative [^{177}Lu] Lu-BiOncoFAP-11 had a longer half-life in tumors besides enhanced tumor uptake and residence time for effective tumor treatment [117].

In addition to its monomeric analogs, the FAP inhibitor dimer (DOTA-2P [FAPI] $_2$) was evaluated as a potential theranostic probe. The pharmacokinetic properties of [^{68}Ga] Ga / [^{177}Lu]Lu-DOTA-2P (FAPI)$_2$ were assessed *via* stability, biodistribution, and radionuclide therapy. Compared with monomeric analogs, DOTA-2P (FAPI) $_2$ has superior retention and uptake of tumors, making FAPI-based vectors extremely valuable for radionuclide therapy and PET imaging. It may also be safe and effective to use [^{177}Lu] Lu-DOTA-2P (FAPI)$_2$ for the treatment of malignant tumors that are FAP-positive [118].

5. Challenges and future perspectives

Using FAP as the theranostic agent to monitor tumor microenvironment changes can provide vital information for identifying cancer-related targets for treatment and prevention. Several types of cancer are overexpressed by FAP, including breast, colorectal, pancreatic, lung, bladder, and ovarian. Although it is undeniable that FAP is present in malignant tissues, the literature has been inconsistent regarding its biological role and its impact on disease outcomes [13]. For instance, FAP's prognostic value in breast cancer is controversial, with some studies showing enhanced FAP is closely related to poorer survival, while others have demonstrated enhanced FAP is closely related to better survival. On the other hand in colorectal and gastric cancer, the high FAP was linked to increased invasion depth, metastases to lymph nodes, and higher grade, as well as a shorter overall survival time [119]. As far as pancreatic cancer is concerned, lower levels of FAP have been associated with more severe pancreatic fibrosis, while higher levels are linked to adverse clinical outcomes like tumor recurrence and metastasis of lymph nodes, as well as death [120]. Furthermore, enhanced FAP expression was strongly associated with fibrotic foci, perineural invasion, tumor size, and patient age. FAP expression, however, has been clearly related to better clinical outcomes in some studies. Cancerous ovarian tumors express FAP, while benign tumors, normal ovarian tissue, and low malignant tumors display no FAP expression. A higher FAP level was also linked with shorter disease-free survival. However, age, histology grade, and tumor type had no significant association with FAP levels. In brain tumors, FDG PET/CT is limited by high physiologic uptake. FAPI PET/CT can be revolutionary in this regard due to its low level of physiological background activity in the brain. Glial tumor's FAP-expression levels are associated with tumor grade. Interestingly, FAP expression is negligible in benign brain lesions and low-grade astrocytomas [121]. Compared to primary brain tumors, metastatic carcinoma lesions expressed FAP [122]. This concept would be challenged in the future by demonstrating whether expression of FAP occurs in high-grade tumors. For example, a glioma study found that increased levels of FAP expression were associated with lower survival, but this could be explained by the fact that FAP is highly expressed in malignant gliomas[121]. Moreover, FAPI uptake with high TBRs was found in isocitrate dehydrogenase (IDH)-wildtype glioblastomas and grade III/IV IDH-mutant glioblastomas. This enabled differentiation between low-grade and high-grade gliomas using FAPI uptake [123]. Despite this, it was unclear whether the heterogeneous uptake pattern in individual tumors resulted from variations in tumor perfusion or from intratumoral asymmetry in FAP expression [124].

Adult healthy tissues show little physiological expression of FAP [125]. Nonetheless, the presence of FAP expression on activated fibroblasts contributing to wound healing, tissue remodeling, fibrosis, degenerative, arthritic processes, and atherosclerosis raises uncertainty about FAPI specificity as a malignancy imaging modality. For instance, non-tumor-specific FAPI uptake is common in degenerative joints and vertebral bones, for example[126]. FAPI PET/CT can be difficult to interpret in gynecological cancers due to variable physiological uterine FAPI uptake [127]. Muscles, scarring, wounds, oral/nasal mucosa, salivary glands, teeth, and mammary glands were other non-tumor-specific sites [78]. Additionally, FAPI is uptaken by benign tumors like pulmonary solitary fibrous tumors,

renal angiomyolipoma, schwannoma, cutaneous fibromas, *etc*. [128–130]. A variety of inflammatory conditions have also been reported to uptake FAPI, including myocarditis, pneumonitis, pleuritis, appendicitis, colitis, and sclerosing cholangitis. [131–133]. Reporting physicians' knowledge of the above-mentioned is crucial to the accurate interpretation of FAPI PET/CT.

Introducing new categories of FAP radiotracers would accelerate the development of radioisotope therapies, which could treat various cancers, including breast, prostate, and brain cancer. Radiation dose prediction and treatment to the maximum tolerated level will also require advanced imaging methods for radioisotope treatment with alpha- and beta-emitters. FAP-targeted radiotracers in individual radioisotope therapy have an excellent chance of gaining widespread acceptance in medicine. FAP-targeted radiotherapy must be adequately supported by scientific evidence over standard radionuclide therapy to achieve this. Table 3 showed the radiolabeled FAPIs that are in Phase II clinical trial.

6. Conclusion

Despite the lack of understanding of FAP's function in malignancies, numerous attempts have been made to exploit the biology of FAP in clinical settings. A new class of radiopharmaceuticals is being developed to visualize tumor stromal FAP with radiolabeled FAP-based inhibitors [19]. FAPI radiotracers have been extensively studied both preclinically and clinically by several research groups in recent years for their potential as cancer diagnostics and therapies [134,135]. Imaging various cancers with ^{68}Ga-labeled FAPI PET and ^{99m}TC-labeled FAPI SPECT appears to be a promising strategy based on current reports [136].

FAPI molecules are not as specific to cancer-associated FAP substrates as they could be. The stability of the interaction and the following clearance depends on the nature of the molecular interaction of the given compound warhead and the FAP. These constraints can hinder targeted radionuclide therapy and cannot provide long-term radiotracer tracking. As a result, FAPI molecules are currently being optimized structurally to improve their pharmacokinetic properties. Even though FAP-targeted therapeutics appear lacking in clinical success, their striking occurrence in many diseases suggests that they may be useful in some clinical settings [137]. It's worth noting that, due to a lack of validated studies, FAP-targeted radiotherapy is ambiguous, whereas the integration of molecular radiotherapy and immunotherapy is more likely to be effective.

Acknowledgment

This work was supported by the Research Center for Pharmaceutical Nanotechnology (RCPN), Tabriz University of Medical Sciences (grant number: 72422).

References

[1]. Whiteside T, The tumor microenvironment and its role in promoting tumor growth, Oncogene 27 (2008) 5904–5912. [PubMed: 18836471]

[2]. Vahidfar N, Aghanejad A, Ahmadzadehfar H, Farzanehfar S, Eppard E, Theranostic advances in breast cancer in nuclear medicine, Int. J. Mol. Sci 22 (9) (2021) 4597. [PubMed: 33925632]

[3]. Aghanejad A, Jalilian AR, Fazaeli Y, Beiki D, Fateh B, Khalaj A, Radiosynthesis and biodistribution studies of [62Zn/62Cu]-plerixafor complex as a novel in vivo PET generator for chemokine receptor imaging, J. Radioanal. Nucl. Chem 299 (2014) 1635–1644.

[4]. Hanahan D, Weinberg RA, Hallmarks of cancer: the next generation, Cell 144 (2011) 646–674. [PubMed: 21376230]

[5]. Öhlund D, Elyada E, Tuveson D, Fibroblast heterogeneity in the cancer wound, J. Exp. Med 211 (2014) 1503–1523. [PubMed: 25071162]

[6]. Neesse A, Algül H, Tuveson DA, Gress TM, Stromal biology and therapy in pancreatic cancer: a changing paradigm, Gut. 64 (2015) 1476–1484. [PubMed: 25994217]

[7]. Smith NR, Baker D, Farren M, Pommier A, Swann R, Wang X, et al. , Tumor stromal architecture aan define the intrinsic tumor response to VEGF-targeted TherapyTumor stromal phenotypes define VEGF sensitivity, Clin. Cancer Res 19 (2013) 6943–6956. [PubMed: 24030704]

[8]. Xing F, Saidou J, Watabe K, Cancer associated fibroblasts (CAFs) in tumor microenvironment, Front. Biosci 15 (2010) 166.

[9]. Aghanejad A, Bonab SF, Sepehri M, Haghighi FS, Tarighatnia A, Kreiter C, et al. , A review on targeting tumor microenvironment: the main paradigm shift in the mAb-based immunotherapy of solid tumors, Int. J. Biol. Macromol 207 (2022) 592–610. [PubMed: 35296439]

[10]. Liu T, Han C, Wang S, Fang P, Ma Z, Xu L, et al. , Cancer-associated fibroblasts: an emerging target of anti-cancer immunotherapy, J. Hematol. Oncol 12 (2019) 1–15. [PubMed: 30606227]

[11]. álvarez-Teijeiro S, García-Inclán C, Villaronga M.á., Casado P, Hermida-Prado F, Granda-Díaz R, et al. , Factors secreted by cancer-associated fibroblasts that sustain cancer stem properties in head and neck squamous carcinoma cells as potential therapeutic targets, Cancers. 10 (2018) 334. [PubMed: 30227608]

[12]. Liu R, Li H, Liu L, Yu J, Ren X, Fibroblast activation protein: a potential therapeutic target in cancer, Cancer Biol. Ther 13 (2012) 123–129. [PubMed: 22236832]

[13]. Fitzgerald AA, Weiner LM, The role of fibroblast activation protein in health and malignancy, Cancer Metastasis Rev. 39 (2020) 783–803. [PubMed: 32601975]

[14]. Lee H-O, Mullins SR, Franco-Barraza J, Valianou M, Cukierman E, Cheng JD, FAP-overexpressing fibroblasts produce an extracellular matrix that enhances invasive velocity and directionality of pancreatic cancer cells, BMC Cancer 11 (2011) 1–13. [PubMed: 21194487]

[15]. Calais J, FAP: the next billion dollar nuclear theranostics target? J. Nucl. Med 61 (2020) 163–165. [PubMed: 31924719]

[16]. Hamson EJ, Keane FM, Tholen S, Schilling O, Gorrell MD, Understanding fibroblast activation protein (FAP): substrates, activities, expression and targeting for cancer therapy, Proteom. - Clin. Appl 8 (2014) 454–463.

[17]. Sandberg TP, Stuart M, Oosting J, Tollenaar R, Sier CFM, Mesker WE, Increased expression of cancer-associated fibroblast markers at the invasive front and its association with tumor-stroma ratio in colorectal cancer, BMC Cancer 19 (2019) 284. [PubMed: 30922247]

[18]. Wu J, Liang C, Chen M, Su W, Association between tumor-stroma ratio and prognosis in solid tumor patients: a systematic review and meta-analysis, Oncotarget. 7 (2016) 68954–68965. [PubMed: 27661111]

[19]. Imlimthan S, Moon ES, Rathke H, Afshar-Oromieh A, Rösch F, Rominger A, et al. , New frontiers in cancer imaging and therapy based on radiolabeled fibroblast activation protein inhibitors: a rational review and current progress, Pharmaceuticals. 14 (2021) 1023. [PubMed: 34681246]

[20]. Gilardi L, Farulla L.S. Airò, Demirci E, Clerici I, Omodeo Salé E, Ceci F, Imaging cancer-associated fibroblasts (CAFs) with FAPi PET, Biomedicines. 10 (2022) 523. [PubMed: 35327325]

[21]. Aghanejad A, Jalilian AR, Fazaeli Y, Alirezapoor B, Pouladi M, Beiki D, et al. , Synthesis and evaluation of [67Ga]-AMD3100: a novel imaging agent for targeting the chemokine receptor CXCR4, Sci. Pharm 82 (2014) 29–42. [PubMed: 24634840]

[22]. Aghanejad A, Jalilian AR, Maus S, Yousefnia H, Geramifar P, Beiki D, Optimized production and quality control of 68Ga-DOTATATE, Iran J. Nucl. Med 24 (2016) 29–36.

[23]. Foroughi-Nia B, Barar J, Memar MY, Aghanejad A, Davaran S, Progresses in polymeric nanoparticles for delivery of tyrosine kinase inhibitors, Life Sci. 278 (2021) 119642. [PubMed: 34033837]

[24]. Mirzaei A, Jalilian AR, Aghanejad A, Mazidi M, Yousefnia H, Shabani G, et al. , Preparation and evaluation of 68Ga-ECC as a PET renal imaging agent, Nucl. Med. Mol. Imaging 49 (2015) 208–216. [PubMed: 26279694]

[25]. Olson MT, Ly QP, Mohs AM, Fluorescence guidance in surgical oncology: challenges, opportunities, and translation, Mol. Imaging Biol 21 (2019) 200–218. [PubMed: 29942988]

[26]. Alam IS, Steinberg I, Vermesh O, van den Berg NS, Rosenthal EL, van Dam GM, et al. , Emerging intraoperative imaging modalities to improve surgical precision, Mol. Imaging Biol 20 (2018) 705–715. [PubMed: 29916118]

[27]. Barth CW, Gibbs SL, Fluorescence image-guided surgery: a perspective on contrast agent development, in: Molecular-guided Surgery: Molecules, Devices, and Applications VI 11222, 2020, pp. 27–42.

[28]. Nabi PN, Vahidfar N, Tohidkia MR, Hamidi AA, Omidi Y, Aghanejad A, Mucin-1 conjugated polyamidoamine-based nanoparticles for image-guided delivery of gefitinib to breast cancer, Int. J. Biol. Macromol 174 (2021) 185–197. [PubMed: 33516855]

[29]. Rüger R, Tansi FL, Rabenhold M, Steiniger F, Kontermann RE, Fahr A, et al. , In vivo near-infrared fluorescence imaging of FAP-expressing tumors with activatable FAP-targeted, single-chain Fv-immunoliposomes, J. Control. Release 186 (2014) 1–10. [PubMed: 24810115]

[30]. Luo H, England CG, Goel S, Graves SA, Ai F, Liu B, et al. , ImmunoPET and near-infrared fluorescence imaging of pancreatic cancer with a dual-labeled bispecific antibody fragment, Mol. Pharm 14 (2017) 1646–1655. [PubMed: 28292180]

[31]. Slania SL, Das D, Lisok A, Du Y, Jiang Z, Mease RC, et al. , Imaging of fibroblast activation protein in cancer xenografts using novel (4-quinolinoyl)-glycyl-2-cyanopyrrolidine-based small molecules, J. Med. Chem 64 (2021) 4059–4070. [PubMed: 33730493]

[32]. Tansi FL, Rüger R, Böhm C, Kontermann RE, Teichgraeber UK, Fahr A, et al. , Potential of activatable FAP-targeting immunoliposomes in intraoperative imaging of spontaneous metastases, Biomaterials. 88 (2016) 70–82. [PubMed: 26945457]

[33]. Tansi FL, Rüger R, Böhm C, Steiniger F, Kontermann RE, Teichgraeber UK, et al. , Activatable bispecific liposomes bearing fibroblast activation protein directed single chain fragment/Trastuzumab deliver encapsulated cargo into the nuclei of tumor cells and the tumor microenvironment simultaneously, Acta Biomater. 54 (2017) 281–293. [PubMed: 28347861]

[34]. Tansi FL, Rüger R, Kollmeier AM, Böhm C, Kontermann RE, Teichgraeber UK, et al. , A fast and effective determination of the biodistribution and subcellular localization of fluorescent immunoliposomes in freshly excised animal organs, BMC Biotechnol. 17 (2017) 1–11. [PubMed: 28056928]

[35]. Tansi FL, Rüger R, Kollmeier AM, Rabenhold M, Steiniger F, Kontermann RE, et al. , Targeting the tumor microenvironment with fluorescence-activatable bispecific endoglin/fibroblast activation protein targeting liposomes, Pharmaceutics. 12 (2020) 370. [PubMed: 32316521]

[36]. Tansi FL, Rüger R, Böhm C, Steiniger F, Raasch M, Mosig AS, et al. , Rapid target binding and cargo release of activatable liposomes bearing HER2 and FAP single-chain antibody fragments reveal potentials for image-guided delivery to tumors, Pharmaceutics. 12 (2020).

[37]. Roy J, Hettiarachchi SU, Kaake M, Mukkamala R, Low PS, Design and validation of fibroblast activation protein alpha targeted imaging and therapeutic agents, Theranostics. 10 (2020) 5778. [PubMed: 32483418]

[38]. Altmann A, Haberkorn U, Siveke J, The latest developments in imaging of fibroblast activation protein, J. Nucl. Med 62 (2021) 160–167. [PubMed: 33127618]

[39]. Hintz HM, Gallant JP, Vander Griend DJ, Coleman IM, Nelson PS, LeBeau AM, Imaging fibroblast activation protein alpha improves diagnosis of metastatic prostate cancer with positron emission tomography imaging FAP in prostate cancer, Clin. Cancer Res 26 (2020) 4882–4891. [PubMed: 32636317]

[40]. Kömek H, Can C, Kaplan İ, Gündoğan C, Kepenek F, Karaoglan H, et al. , Comparison of [68 Ga] Ga-DOTA-FAPI-04 PET/CT and [18F] FDG PET/CT in colorectal cancer, Eur. J. Nucl. Med. Mol. Imaging (2022) 1–12. [PubMed: 36251026]

[41]. Wei Y, Zheng J, Ma L, Liu X, Xu S, Wang S, et al. , [18F] AlF-NOTA-FAPI-04: FAP-targeting specificity, biodistribution, and PET/CT imaging of various cancers, Eur. J. Nucl. Med. Mol. Imaging (2022) 1–13. [PubMed: 36251026]

[42]. Kou Y, Jiang X, Yao Y, Shen J, Jiang X, Chen S, et al. , Physiological tracer distribution and benign lesion incidental uptake of Al18F-NOTA-FAPI-04 on PET/CT imaging, Nucl. Med. Commun 10 (1097) (2022).

[43]. Qin C, Shao F, Gai Y, Liu Q, Ruan W, Liu F, et al. , 68Ga-DOTA-FAPI-04 PET/MR in the evaluation of gastric carcinomas: comparison with 18F-FDG PET/CT, J. Nucl. Med 63 (2022) 81–88. [PubMed: 33863819]

[44]. de Galiza Barbosa F, Queiroz MA, Nunes RF, Costa LB, Zaniboni EC, Marin JFG, et al. , Nonprostatic diseases on PSMA PET imaging: a spectrum of benign and malignant findings, Cancer Imaging 20 (2020) 1–23.

[45]. Kratochwil C, Flechsig P, Lindner T, Abderrahim L, Altmann A, Mier W, et al. , 68Ga-FAPI PET/CT: tracer uptake in 28 different kinds of cancer, J. Nucl. Med 60 (2019) 801–805. [PubMed: 30954939]

[46]. Hu K, Li L, Huang Y, Ye S, Zhong J, Yan Q, et al. , Radiosynthesis and preclinical evaluation of bispecific PSMA/FAP heterodimers for tumor imaging, Pharmaceuticals. 15 (2022) 383. [PubMed: 35337180]

[47]. Zhang Q, Lin X, Wang W, Zhang X, Lü M, Shao Z, et al. , Evaluation of 18F-FAPI-04 imaging in assessing the therapeutic response of rheumatoid arthritis, Mol. Imaging Biol (2023) 1–8.

[48]. Huang J, Fu L, Zhang X, Huang S, Dong Y, Hu K, et al. , Noninvasive imaging of FAP expression using positron emission tomography: a comparative evaluation of a [18F]-labeled glycopeptide-containing FAPI with [18F] FAPI-42, Eur. J. Nucl. Med. Mol. Imaging (2023) 1–12.

[49]. Giesel FL, Adeberg S, Syed M, Lindner T, Jiménez-Franco LD, Mavriopoulou E, et al. , FAPI-74 PET/CT using either 18F-AlF or cold-kit 68Ga labeling: biodistribution, radiation dosimetry, and tumor delineation in lung cancer patients, J. Nucl. Med 62 (2021) 201–207. [PubMed: 32591493]

[50]. Toms J, Kogler J, Maschauer S, Daniel C, Schmidkonz C, Kuwert T, et al. , Targeting fibroblast activation protein: radiosynthesis and preclinical evaluation of an 18F-labeled FAP inhibitor, J. Nucl. Med 61 (2020) 1806–1813. [PubMed: 32332144]

[51]. Greifenstein L, Kramer CS, Moon ES, Rösch F, Klega A, Landvogt C, et al. , From automated synthesis to in vivo application in multiple types of cancer—clinical results with [68Ga] Ga-DATA5m. SA. FAPi, Pharmaceuticals 15 (2022) 1000. [PubMed: 36015148]

[52]. Xie Z, Yang W, Wang J, 68Ga-PSMA-FAPI PET imaging of prostate cancer with negative or low PSMA expression, Soc. Nuclear Med 63 (2022) 2832.

[53]. Liu Z, Wang F, Chen X, Integrin αvβ3-targeted cancer therapy, Drug Dev. Res 69 (2008) 329–339. [PubMed: 20628538]

[54]. Chen X, Hou Y, Tohme M, Park R, Khankaldyyan V, Gonzales-Gomez I, et al. , Pegylated Arg-Gly-Asp peptide: 64Cu labeling and PET imaging of brain tumor αvβ3-integrin expression, J. Nucl. Med 45 (2004) 1776–1783. [PubMed: 15471848]

[55]. Chen X, Park R, Shahinian AH, Bading JR, Conti PS, Pharmacokinetics and tumor retention of 125I-labeled RGD peptide are improved by PEGylation, Nucl. Med. Biol 31 (2004) 11–19. [PubMed: 14741566]

[56]. Li Z-B, Wu Z, Chen K, Ryu EK, Chen X, 18F-labeled BBN-RGD heterodimer for prostate cancer imaging, J. Nucl. Med 49 (2008) 453–461. [PubMed: 18287274]

[57]. Zang J, Wen X, Lin R, Zeng X, Wang C, Shi M, et al. , Synthesis, preclinical evaluation and radiation dosimetry of a dual targeting PET tracer [68Ga] Ga-FAPI-RGD, Theranostics. 12 (2022) 7180–7190. [PubMed: 36276644]

[58]. Zhao L, Wen X, Xu W, Pang Y, Sun L, Wu X, et al. , Clinical evaluation of 68Ga-FAPI-RGD for imaging of fibroblast activation protein and integrin αvβ3 in various cancer types, J. Nucl. Med 64 (2023), 122.265383.

[59]. Mona CE, Benz MR, Hikmat F, Grogan TR, Lueckerath K, Razmaria A, et al. , Correlation of 68Ga-FAPi-46 PET biodistribution with FAP expression by immunohistochemistry in patients with solid cancers: interim analysis of a prospective translational exploratory study, J. Nucl. Med 63 (2022) 1021–1026. [PubMed: 34740953]

[60]. Unterrainer LM, Lindner S, Eismann L, Casuscelli J, Gildehaus F-J, Bui VN, et al. , Feasibility of [68Ga] Ga-FAPI-46 PET/CT for detection of nodal and hematogenous spread in high-grade urothelial carcinoma, Eur. J. Nucl. Med. Mol. Imaging (2022) 1–10. [PubMed: 36251026]

[61]. Siripongsatian D, Promteangtrong C, Kunawudhi A, Kiatkittikul P, Boonkawin N, Chinnanthachai C, et al. , Comparisons of quantitative parameters of Ga-68-labelled fibroblast activating protein inhibitor (FAPI) PET/CT and [18F] F-FDG PET/CT in patients with liver malignancies, Mol. Imaging Biol (2022) 1–12.

[62]. Zhang H, An J, Wu P, Zhang C, Zhao Y, Tan D, et al. , The application of [68Ga]-labeled FAPI-04 PET/CT for targeting and early detection of pancreatic carcinoma in patient-derived orthotopic xenograft models, Contrast Media Mol. Imaging 2022 (2022).

[63]. Lan L, Liu H, Wang Y, Deng J, Peng D, Feng Y, et al. , The potential utility of [68 Ga] Ga-DOTA-FAPI-04 as a novel broad-spectrum oncological and non-oncological imaging agent—comparison with [18F] FDG, Eur. J. Nucl. Med. Mol. Imaging 49 (2022) 963–979. [PubMed: 34410435]

[64]. Ding J, Qiu J, Hao Z, Huang H, Liu Q, Liu W, et al. , Prognostic value of preoperative [68 Ga] Ga-FAPI-04 PET/CT in patients with resectable pancreatic ductal adenocarcinoma in correlation with immunohistological characteristics, Eur. J. Nucl. Med. Mol. Imaging (2023) 1–12.

[65]. Kim S-K, Chung J-K, Kim BT, Kim SJ, Jeong JM, Lee DS, et al. , Relationship between gastrointestinal F-18-fluorodeoxyglucose accumulation and gastrointestinal symptoms in whole-body PET, Clinical Positron Imaging 2 (1999) 273–279. [PubMed: 14516651]

[66]. Prabhakar HB, Sahani DV, Fischman AJ, Mueller PR, Blake MA, Bowel hot spots at PET-CT, Radiographics. 27 (2007) 145–159. [PubMed: 17235004]

[67]. Shangguan C, Yang C, Shi Z, Miao Y, Hai W, Shen Y, et al., 68Ga-FAPI-04 PET Distinguishes Malignancy from Inflammatory Lesions, 2022.

[68]. Qi N, Wang H, Wang H, Ren S, You Z, Chen X, et al. , Non-tumoral uptake of 68Ga-FAPI-04 PET: a retrospective study, Front. Oncol 12 (2022).

[69]. Zhang M, Quan W, Zhu T, Feng S, Huang X, Meng H, et al. , [68Ga]Ga-DOTA-FAPI-04 PET/MR in patients with acute myocardial infarction: potential role of predicting left ventricular remodeling, Eur. J. Nucl. Med. Mol. Imaging 50 (2023) 839–848. [PubMed: 36326870]

[70]. Zhou X, Wang S, Xu X, Meng X, Zhang H, Zhang A, et al. , Higher accuracy of [68 Ga] Ga-DOTA-FAPI-04 PET/CT comparing with 2-[18F] FDG PET/CT in clinical staging of NSCLC, Eur. J. Nucl. Med. Mol. Imaging (2022) 1–11. [PubMed: 36251026]

[71]. Pang Y, Zhao L, Meng T, Xu W, Lin Q, Wu H, et al. , PET imaging of fibroblast activation protein in various types of cancers by using 68Ga-FAP-2286: comparison with 18F-FDG and 68Ga-FAPI-46 in a single-center, prospective study, J. Nucl. Med 64 (2023) 386–394. [PubMed: 36215571]

[72]. Pang Y, Zhao L, Meng T, Xu W, Lin Q, Wu H, et al. , PET imaging of fibroblast activation protein in various types of cancer using 68Ga-FAP-2286: comparison with 18F-FDG and 68Ga-FAPI-46 in a single-center, prospective study, J. Nucl. Med 64 (2023) 386–394. [PubMed: 36215571]

[73]. Guberina N, Kessler L, Pöttgen C, Guberina M, Metzenmacher M, Herrmann K, et al. , [68Ga] FAPI-PET/CT for radiation therapy planning in biliary tract, pancreatic ductal adeno-, and adenoidcystic carcinomas, Sci. Rep 12 (2022) 1–14. [PubMed: 34992227]

[74]. Luo Y, Pan Q, Yang H, Peng L, Zhang W, Li F, Fibroblast activation protein–targeted PET/CT with 68Ga-FAPI for imaging IgG4-related disease: comparison to 18F-FDG PET/CT, J. Nucl. Med 62 (2021) 266–271. [PubMed: 32513902]

[75]. Schmidkonz C, Rauber S, Atzinger A, Agarwal R, Götz TI, Soare A, et al. , Disentangling inflammatory from fibrotic disease activity by fibroblast activation protein imaging, Ann. Rheum. Dis 79 (2020) 1485–1491. [PubMed: 32719042]

[76]. Glatting FM, Hoppner J, Liew DP, van Genabith A, Spektor A-M, Steinbach L, et al. , Repetitive early FAPI-PET acquisition comparing FAPI-02, FAPI-46 and FAPI-74: methodological and diagnostic implications for malignant, inflammatory and degenerative lesions, J. Nucl. Med (2022), 122.264069.

[77]. Roth KS, Voltin C-A, van Heek L, Wegen S, Schomäcker K, Fischer T, et al. , Dual-tracer PET/CT protocol with [18F]-FDG and [68Ga] Ga-FAPI-46 for cancer imaging: a proof of concept, J. Nucl. Med 63 (2022) 1683–1686. [PubMed: 35422446]

[78]. Kessler L, Ferdinandus J, Hirmas N, Zarrad F, Nader M, Kersting D, et al. , Pitfalls and common findings in 68Ga-FAPI PET: a pictorial analysis, J. Nucl. Med 63 (2022) 890–896. [PubMed: 34620730]

[79]. Gündogan C, Güzel Y, Can C, Alabalik U, Kömek H, False-positive 68ga–fibroblast activation protein-specific inhibitor uptake of benign lymphoid tissue in a patient with breast cancer, Clin. Nucl. Med 46 (2021), e433–e5. [PubMed: 33782295]

[80]. Wu J, Wang Y, Liao T, Rao Z, Gong W, Ou L, et al. , Comparison of the relative diagnostic performance of [68Ga] Ga-DOTA-FAPI-04 and [18F] FDG PET/CT for the detection of bone metastasis in patients with different cancers, Front. Oncol 11 (2021) 737827. [PubMed: 34604078]

[81]. Verena A, Kuo H-T, Merkens H, Zeisler J, Bendre S, Wong AA, et al. , Novel 68Ga-labeled pyridine-based fibroblast activation protein-targeted tracers with high tumor-to-background contrast, Pharmaceuticals. 16 (2023) 449. [PubMed: 36986548]

[82]. Trujillo-Benítez D, Luna-Gutiérrez M, Ferro-Flores G, Ocampo-García B, Santos-Cuevas C, Bravo-Villegas G, et al. , Design, synthesis and preclinical assessment of 99mTc-iFAP for in vivo fibroblast activation protein (FAP) imaging, Molecules. 27 (2022) 264. [PubMed: 35011496]

[83]. Jiang Y, Tian Y, Feng B, Zhao T, Du L, Yu X, et al. , A novel molecular imaging probe [99mTc] Tc-HYNIC-FAPI targeting cancer-associated fibroblasts, Sci. Rep 13 (2023) 3700. [PubMed: 36879039]

[84]. Luo X, Zhang Z, Cheng C, Wang T, Fang D, Zuo C, et al. , SPECT imaging with Tc-99m-labeled HYNIC-FAPI-04 to extend the differential time window in evaluating tumor fibrosis, Pharmaceuticals. 16 (2023) 423. [PubMed: 36986521]

[85]. Vallejo-Armenta P, Ferro-Flores G, Santos-Cuevas C, García-Pérez FO, Casanova-Triviño P, Sandoval-Bonilla B, et al. , [99mTc] Tc-iFAP/SPECT tumor stroma imaging: acquisition and analysis of clinical images in six different cancer entities, Pharmaceuticals 15 (2022) 729. [PubMed: 35745648]

[86]. Coria-Domínguez L, Vallejo-Armenta P, Luna-Gutiérrez M, Ocampo-García B, Gibbens-Bandala B, García-Pérez F, et al. , [99mTc] Tc-iFAP radioligand for SPECT/CT imaging of the tumor microenvironment: kinetics, radiation dosimetry, and imaging in patients, Pharmaceuticals 15 (2022) 590. [PubMed: 35631416]

[87]. Ruan Q, Wang Q, Jiang Y, Feng J, Yin G, Zhang J, Synthesis and evaluation of 99mTc-labeled FAP inhibitors with different linkers for imaging of fibroblast activation proteins in tumors, J. Med. Chem 66 (2023) 4952–4960. [PubMed: 36972467]

[88]. Ruan Q, Zhou C, Wang Q, Kang F, Jiang Y, Li G, et al. , A simple kit formulation for preparation and exploratory human studies of a novel 99mTc-labeled fibroblast activation protein inhibitor tracer for imaging of the fibroblast activation protein in cancers, Mol. Pharm 20 (2023) 2942–2950. [PubMed: 37083360]

[89]. Bendre S, Zhang Z, Colpo N, Zeisler J, Benard F, Lin K-S, Synthesis, radiolabeling and in vivo evaluation of a 99mTc-labeled SPECT tracer for FAP imaging, Soc. Nuclear Med 63 (2022) 2896.

[90]. Lindner T, Altmann A, Krämer S, Kleist C, Loktev A, Kratochwil C, et al. , Design and development of 99mTc-labeled FAPI tracers for SPECT imaging and 188Re therapy, J. Nucl. Med 61 (2020) 1507–1513. [PubMed: 32169911]

[91]. Ruan Q, Feng J, Jiang Y, Zhang X, Duan X, Wang Q, et al. , Preparation and bioevaluation of 99mTc-labeled FAP inhibitors as tumor radiotracers to target the fibroblast activation protein, Mol. Pharm 19 (2021) 160–171. [PubMed: 34904839]

[92]. Wen X, Xu P, Shi M, Liu J, Zeng X, Zhang Y, et al. , Evans blue-modified radiolabeled fibroblast activation protein inhibitor as long-acting cancer therapeutics, Theranostics. 12 (2022) 422. [PubMed: 34987657]

[93]. Wen X, Xu P, Shi M, Guo Z, Zhang X, Khong P-L, et al. , 177Lu-DOTA-EB-FAPI imaging and therapy of fibroblast activation protein (FAP) positive tumors, Soc. Nuclear Med 63 (2022) 4017.

[94]. Zhang P, Xu M, Ding J, Chen J, Zhang T, Huo L, et al. , Fatty acid-conjugated radiopharmaceuticals for fibroblast activation protein-targeted radiotherapy, Eur. J. Nucl. Med. Mol. Imaging 49 (2022) 1985–1996. [PubMed: 34746969]

[95]. Zhao L, Pang Y, Fu K, Guo Z, Sun L, Lin Q, et al. , Development of fibroblast activation protein inhibitor-based dimeric radiotracers with improved tumor uptake and retention, Soc. Nuclear Med 63 (2022) 4044.

[96]. Ballal S, Yadav MP, Moon ES, Kramer VS, Roesch F, Kumari S, et al. , First-in-human results on the biodistribution, pharmacokinetics, and dosimetry of [177Lu] Lu-DOTA. SA. FAPi and [177Lu] Lu-DOTAGA.(SA. FAPi) 2, Pharmaceuticals 14 (2021) 1212. [PubMed: 34959613]

[97]. Zboralski D, Hoehne A, Bredenbeck A, Schumann A, Nguyen M, Schneider E, et al. , Preclinical evaluation of FAP-2286 for fibroblast activation protein targeted radionuclide imaging and therapy, Eur. J. Nucl. Med. Mol. Imaging (2022) 1–17. [PubMed: 36251026]

[98]. Ma H, Li F, Shen G, Cai H, Liu W, Lan T, et al. , Synthesis and preliminary evaluation of 131I-labeled FAPI tracers for cancer theranostics, Mol. Pharm 18 (2021) 4179–4187. [PubMed: 34591481]

[99]. Louault K, Bonneaud T, Séveno C, Gomez-Bougie P, Nguyen F, Gautier F, et al. , Interactions between cancer-associated fibroblasts and tumor cells promote MCL-1 dependency in estrogen receptor-positive breast cancers, Oncogene 38 (2019) 3261–3273. [PubMed: 30631150]

[100]. Loktev A, Lindner T, Mier W, Debus J, Altmann A, Jäger D, et al. , A tumor-imaging method targeting cancer-associated fibroblasts, J. Nucl. Med 59 (2018) 1423–1429. [PubMed: 29626120]

[101]. Lindner T, Loktev A, Altmann A, Giesel F, Kratochwil C, Debus J, et al. , Development of quinoline-based theranostic ligands for the targeting of fibroblast activation protein, J. Nucl. Med 59 (2018) 1415–1422. [PubMed: 29626119]

[102]. Ma H, Li F, Shen G, Pan L, Liu W, Liang R, et al. , In vitro and in vivo evaluation of 211At-labeled fibroblast activation protein inhibitor for glioma treatment, Bioorg. Med. Chem 55 (2022) 116600. [PubMed: 34999526]

[103]. Xu J, Li S, Xu S, Dai J, Luo Z, Cui J, et al. , Screening and preclinical evaluation of novel radiolabeled anti-fibroblast activation protein-α recombinant antibodies, Cancer Biother. Radiopharm (2022), 10.1089/cbr.2021.0389.

[104]. Watabe T, Liu Y, Kaneda-Nakashima K, Shirakami Y, Lindner T, Ooe K, et al. , Theranostics targeting fibroblast activation protein in the tumor stroma: 64Cu- and 225Ac-labeled FAPI-04 in pancreatic cancer xenograft mouse models, J. Nucl. Med 61 (2020) 563–569. [PubMed: 31586001]

[105]. Li M, Younis MH, Zhang Y, Cai W, Lan X, Clinical summary of fibroblast activation protein inhibitor-based radiopharmaceuticals: cancer and beyond, Eur. J. Nucl. Med. Mol. Imaging 49 (2022) 2844–2868. [PubMed: 35098327]

[106]. Younis MH, Malih S, Lan X, Rasaee MJ, Cai W, Enhancing fibroblast activation protein (FAP)-targeted radionuclide therapy with albumin binding, and beyond, Eur. J. Nucl. Med. Mol. Imaging 49 (2022) 1773–1777. [PubMed: 35332379]

[107]. Millul J, Koepke L, Haridas GR, Sparrer KM, Mansi R, Fani M, Head-to-head comparison of different classes of FAP radioligands designed to increase tumor residence time: monomer, dimer, albumin binders, and small molecules vs peptides, Eur. J. Nucl. Med. Mol. Imaging (2023) 1–12.

[108]. Yang T, Peng L, Qiu J, He X, Zhang D, Wu R, et al. , A radiohybrid theranostics ligand labeled with fluorine-18 and lutetium-177 for fibroblast activation protein-targeted imaging and radionuclide therapy, Eur. J. Nucl. Med. Mol. Imaging (2023) 1–11.

[109]. Aso A, Nabetani H, Matsuura Y, Kadonaga Y, Shirakami Y, Watabe T, et al. , Evaluation of astatine-211-labeled fibroblast activation protein inhibitor (FAPI): comparison of different linkers with polyethylene glycol and piperazine, Int. J. Mol. Sci 24 (2023) 8701. [PubMed: 37240044]

[110]. Becker K, Schwartz P, Aluicio-Sarduy E, Jeffery J, Massey C, Hernandez R, et al. , Preclinical evaluation of 43Sc-FAPI PET for detection of pancreatic ductal adenocarcinoma, Soc. Nuclear Med 63 (2022) 2616.

[111]. Meng L, Fang J, Zhao L, Wang T, Yuan P, Zhao Z, et al. , Rational design and pharmacomodulation of protein-binding theranostic radioligands for targeting the fibroblast activation protein, J. Med. Chem 65 (2022) 8245–8257. [PubMed: 35658448]

[112]. Rami-Mark C, Berroterán-Infante N, Philippe C, Foltin S, Vraka C, Hoepping A, et al. , Radiosynthesis and first preclinical evaluation of the novel norepinephrine transporter pet-ligand [11C] ME@ HAPTHI, EJNMMI Res. 5 (2015) 1–12. [PubMed: 25853007]

[113]. Boinapally S, Lisok A, Lofland G, Minn I, Yan Y, Jiang Z, et al. , Hetero-bivalent agents targeting FAP and PSMA, Eur. J. Nucl. Med. Mol. Imaging 49 (2022) 4369–4381. [PubMed: 35965291]

[114]. Bartoli F, Elsinga P, Nazario LR, Zana A, Galbiati A, Millul J, et al., Automated Radiolabelling Procedures for the Preparation of OncoFAP-based Radiopharmaceuticals for Cancer Imaging and Therapy, 2022.

[115]. Millul J, Bassi G, Mock J, Elsayed A, Pellegrino C, Zana A, et al. , An ultra-high-affinity small organic ligand of fibroblast activation protein for tumor-targeting applications, Proc. Natl. Acad. Sci 118 (2021), e2101852118. [PubMed: 33850024]

[116]. Galbiati A, Zana A, Bocci M, Millul J, Elsayed A, Mock J, et al. , A dimeric FAP-targeting small molecule-radio conjugate with high and prolonged tumour uptake, J. Nucl. Med 63 (2022) 1852–1858. [PubMed: 35589404]

[117]. Puglioli S, Schmidt E, Pellegrino C, Prati L, Oehler S, De Luca R, et al. , Selective tumor targeting enabled by picomolar fibroblast activation protein inhibitors isolated from a DNA-encoded affinity maturation library, Chem. 9 (2023) 411–429.

[118]. Zhao L, Chen J, Pang Y, Fang J, Fu K, Meng L, et al. , Development of fibroblast activation protein inhibitor-based dimeric radiotracers with improved tumor retention and antitumor efficacy, Mol. Pharm 19 (2022) 3640–3651. [PubMed: 35917335]

[119]. Wikberg ML, Edin S, Lundberg IV, Van Guelpen B, Dahlin AM, Rutegård J, et al. , High intratumoral expression of fibroblast activation protein (FAP) in colon cancer is associated with poorer patient prognosis, Tumor Biol. 34 (2013) 1013–1020.

[120]. Kawase T, Yasui Y, Nishina S, Hara Y, Yanatori I, Tomiyama Y, et al. , Fibroblast activation protein-α-expressing fibroblasts promote the progression of pancreatic ductal adenocarcinoma, BMC Gastroenterol. 15 (2015) 1–9. [PubMed: 25609176]

[121]. Matrasova I, Busek P, Balaziova E, Sedo A, Heterogeneity of molecular forms of dipeptidyl peptidase-IV and fibroblast activation protein in human glioblastomas, Biomed. Pap. Med. Fac. Univ. Palacky Olomouc 161 (2017).

[122]. Mentlein R, Hattermann K, Hemion C, Jungbluth AA, Held-Feindt J, Expression and Role of the Cell Surface Protease Seprase/Fibroblast Activation Protein-α (FAP-α) in Astroglial Tumors, 2011.

[123]. Röhrich M, Loktev A, Wefers AK, Altmann A, Paech D, Adeberg S, et al. , IDH-wildtype glioblastomas and grade III/IV IDH-mutant gliomas show elevated tracer uptake in fibroblast activation protein–specific PET/CT, Eur. J. Nucl. Med. Mol. Imaging 46 (2019) 2569–2580. [PubMed: 31388723]

[124]. Chandekar KR, Prashanth A, Vinjamuri S, Kumar R, FAPI PET/CT imaging—an updated review, Diagnostics 13 (2023) 2018. [PubMed: 37370912]

[125]. Lindner T, Loktev A, Giesel F, Kratochwil C, Altmann A, Haberkorn U, Targeting of activated fibroblasts for imaging and therapy, EJNMMI Radiopharm. Chem 4 (2019) 1–15. [PubMed: 31659497]

[126]. Kessler L, Ferdinandus J, Hirmas N, Zarrad F, Nader M, Kersting D, et al. , Pitfalls and common findings in (68)Ga-FAPI PET: a pictorial analysis, J. Nucl. Med 63 (2022) 890–896. [PubMed: 34620730]

[127]. Dendl K, Koerber SA, Finck R, Mokoala KMG, Staudinger F, Schillings L, et al. , (68)Ga-FAPI-PET/CT in patients with various gynecological malignancies, Eur. J. Nucl. Med. Mol. Imaging 48 (2021) 4089–4100. [PubMed: 34050777]

[128]. Guo YH, Yang MF, Increased 18F-ALF-NOTA-FAPI and 18F-FDG uptake in renal Angiomyolipoma, Clin. Nucl. Med 47 (2022), e306–e10. [PubMed: 35025794]

[129]. Wu J, Wang Y, Zhang C, Increased 68Ga-FAPI uptake in neurofibromatosis in a patient with pleomorphic rhabdomyosarcoma, Clin. Nucl. Med 46 (2021) 1018–1019. [PubMed: 34034317]

[130]. Zhu Y, Wu J, Wang Y, Geng J, Zhang C, Presacral benign schwannoma mimics malignancy on 18F-FDG and 68Ga-FAPI PET/CT, Clin. Nucl. Med 47 (2022) 277–278. [PubMed: 34653050]

[131]. Finke D, Heckmann MB, Herpel E, Katus HA, Haberkorn U, Leuschner F, et al. , Early detection of checkpoint inhibitor-associated myocarditis using (68)Ga-FAPI PET/CT, Front. Cardiovasc. Med 8 (2021) 614997. [PubMed: 33718446]

[132]. Tang W, Wu J, Yang S, Wang Q, Chen Y, Organizing pneumonia with intense 68Ga-FAPI uptake mimicking lung cancer on 68Ga-FAPI PET/CT, Clin. Nucl. Med 47 (2022) 223–225. [PubMed: 34392279]

[133]. Yang X, Huang Y, Mou C, Liu H, Chen Y, Chronic colitis mimicking malignancy on 68Ga-FAPI PET/CT, Clin. Nucl. Med 47 (2022) 159–160. [PubMed: 34238800]

[134]. Chandekar KR, Prashanth A, Vinjamuri S, Kumar R, FAPI PET/CT imaging—an updated review, Diagnostics 13 (2023) 2018. [PubMed: 37370912]

[135]. Sidrak MM, De Feo MS, Corica F, Gorica J, Conte M, Filippi L, et al. , Fibroblast activation protein inhibitor (FAPI)-based theranostics—where we are at and where we are heading: a systematic review, Int. J. Mol. Sci 24 (2023) 3863. [PubMed: 36835275]

[136]. Wu Z, Hua Y, Shen Q, Yu C, Research progress on the role of fibroblast activation protein in diagnosis and treatment of cancer, Nucl. Med. Commun 43 (2022) 746–755. [PubMed: 35506275]

[137]. Gilardi L, Airò Farulla LS, Demirci E, Clerici I, Omodeo Salè E, Ceci F, Imaging Cancer-Associated Fibroblasts (CAFs) with FAPi PET, 2022, p. 10.

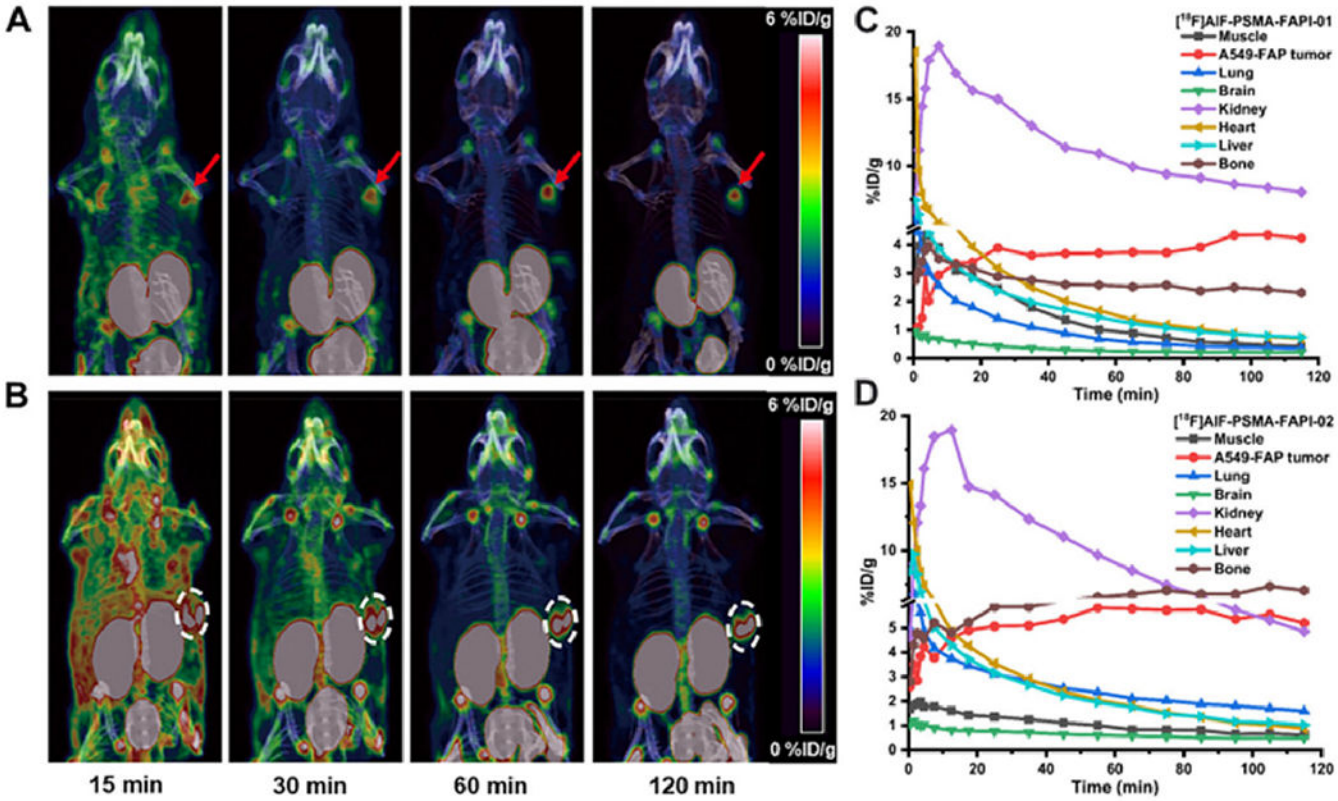

Fig. 1.

PET images were taken 120, 60, 30 and 15 min following injection of (A) [^{18}F] AlF-PSMA-FAPI-01 and (B) [^{18}F]AlF-PSMA-FAPI-02. Time-activity curves up to 120 min later, (C) [^{18}F]AlF-PSMA-FAPI-01 and (D) [^{18}F]AlF-PSMA-FAPI-02. Adapted from ref. [46].

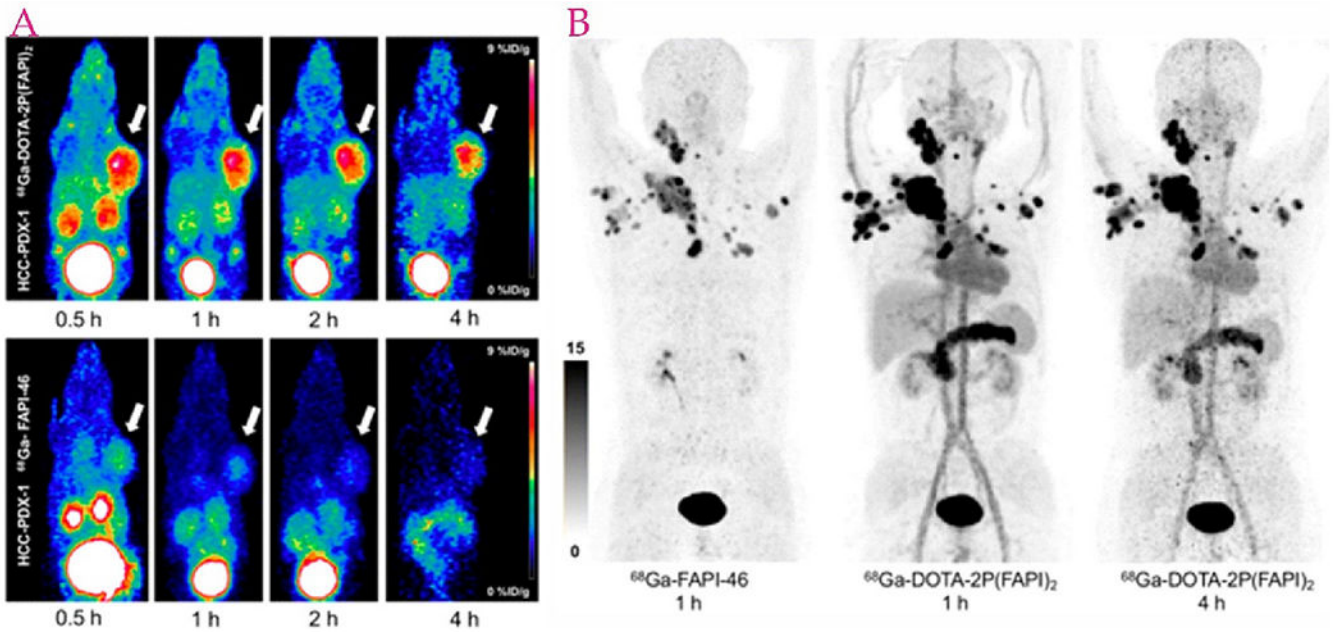

Fig. 2.

A) PET images of HCC-PDX-1, ^{68}Ga-DOTA-2P $(FAPI)_2$ (left top) and ^{68}Ga-FAPI-46 (left bottom). B) PET images of a thyroid cancer patient, ^{68}Ga-FAPI-46 (left, one h after injection) and ^{68}Ga-DOTA-2P $(FAPI)_2$ (right, one and four h after injection). Adapted from ref. [42].

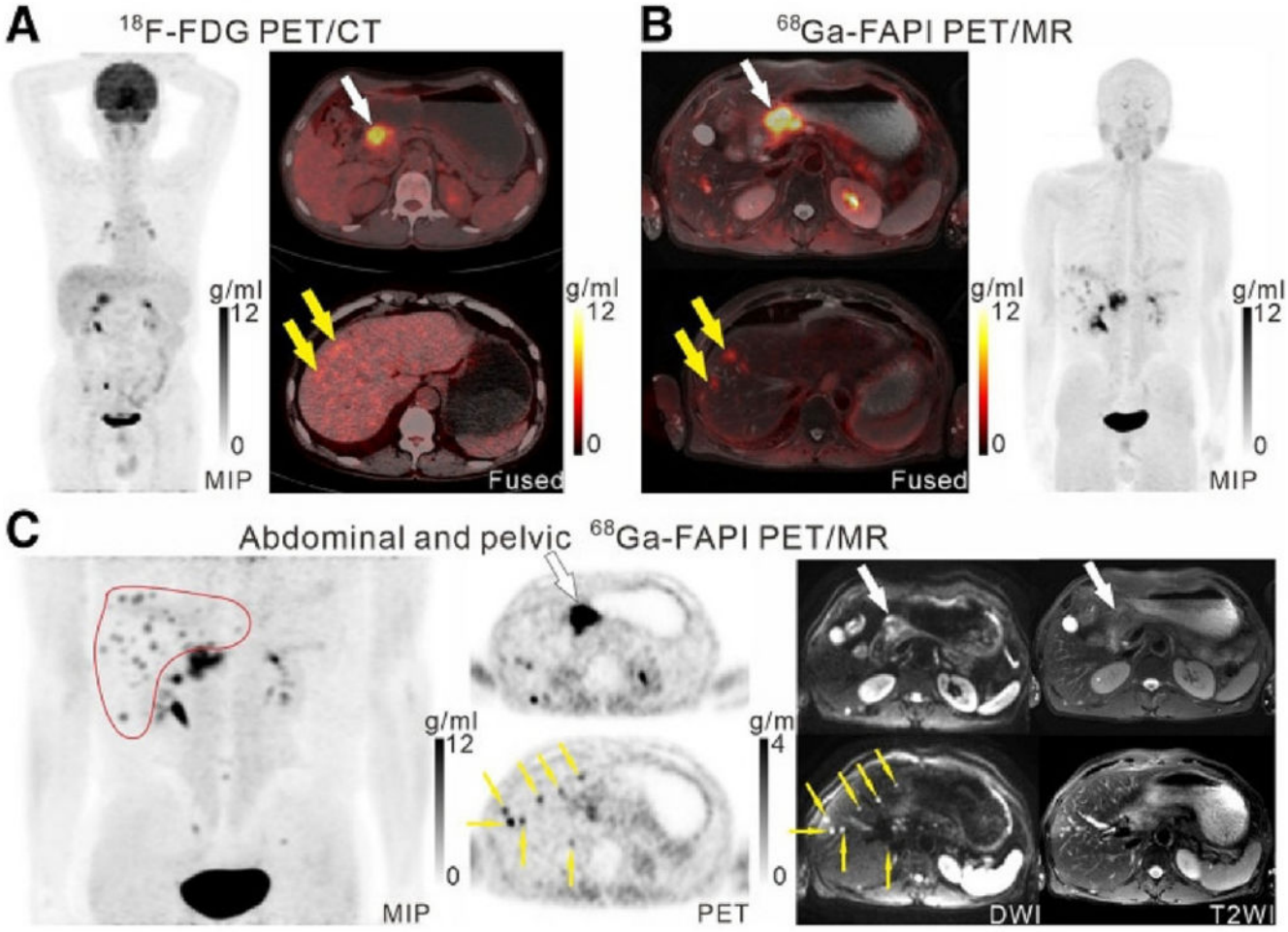

Fig. 3.

Patient with moderately differentiated gastric adenocarcinoma. On ^{18}F-FDG PET/CT images, two foci of abnormal liver activity were observed along with the primary tumor (A, white arrows). PET/MR images of ^{68}Ga-FAPI revealed a high uptake of the primary tumor (B and C), and extensive accumulations of ^{68}Ga-FAPI in the 2 hepatic lesions (B, yellow arrows). Liver (C, red outline, yellow arrows) also exhibited several foci of ^{68}Ga-FAPI enhancement that coincided with strong DWI signals (yellow arrows), indicating liver metastases in multiple locations. Adapted from ref. [43].

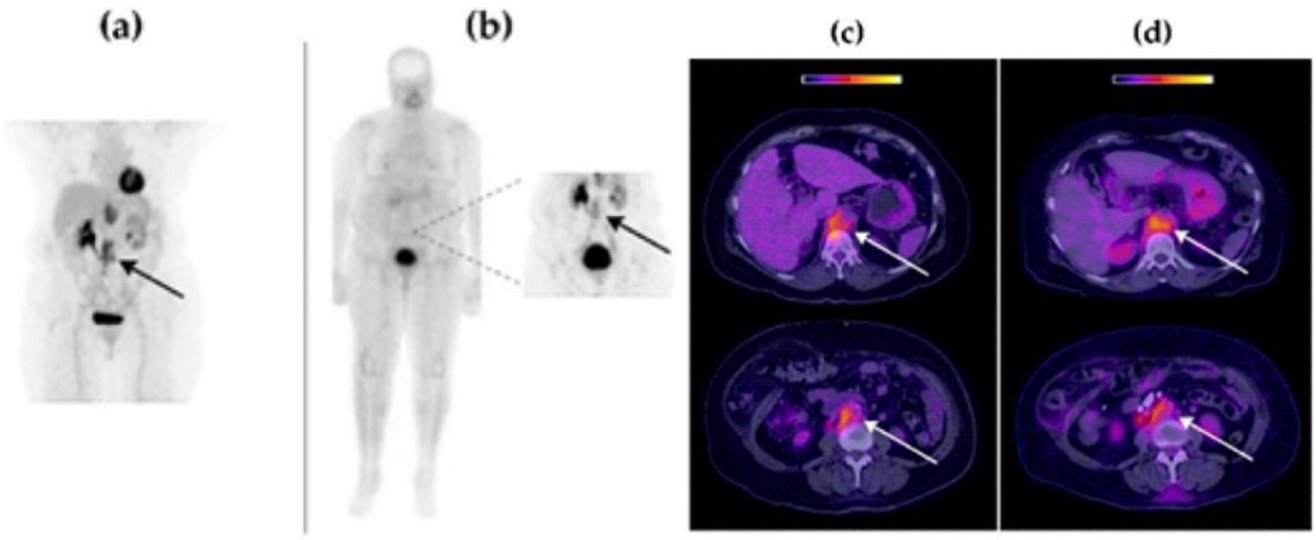

Fig. 4.

Retroperitoneal lymph node recurrence in a patient with cervical squamous cell carcinoma. (a and c) PET image of [^{18}F] FDG one hour after injection, (b and d) SPECT image of [^{99m}Tc] Tc-FAPI three hour after injection. In all tumor lesions, both radiopharmaceuticals were absorbed similarly Adapted from ref. [86].

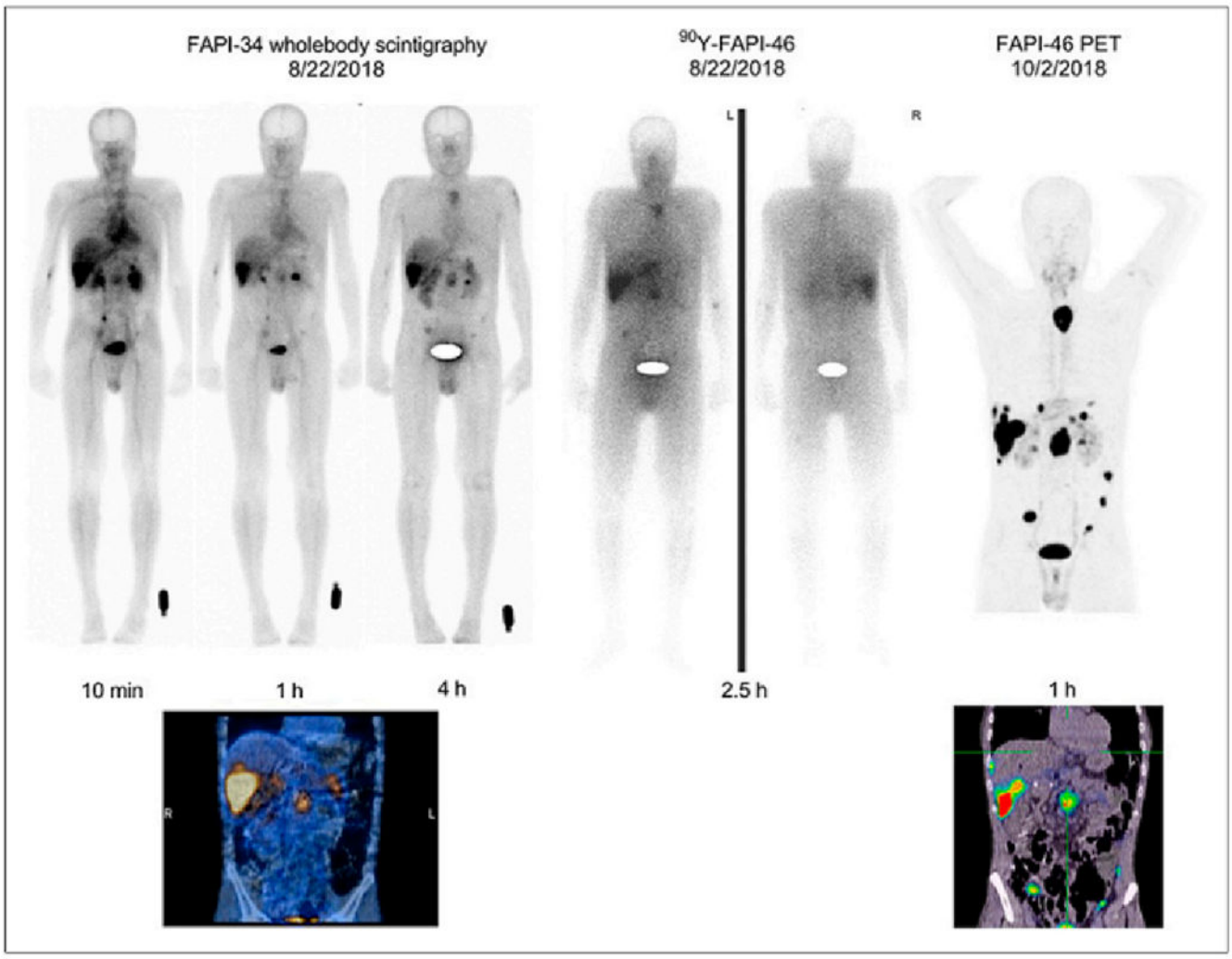

Fig. 5.

Intra-therapeutic imaging with ^{99m}Tc-labeled FAPI-34 during pancreatic cancer treatment with ^{68}Ga-labeled FAPI-46 and ^{90}Y-FAPI-46. Adapted from ref. [90].

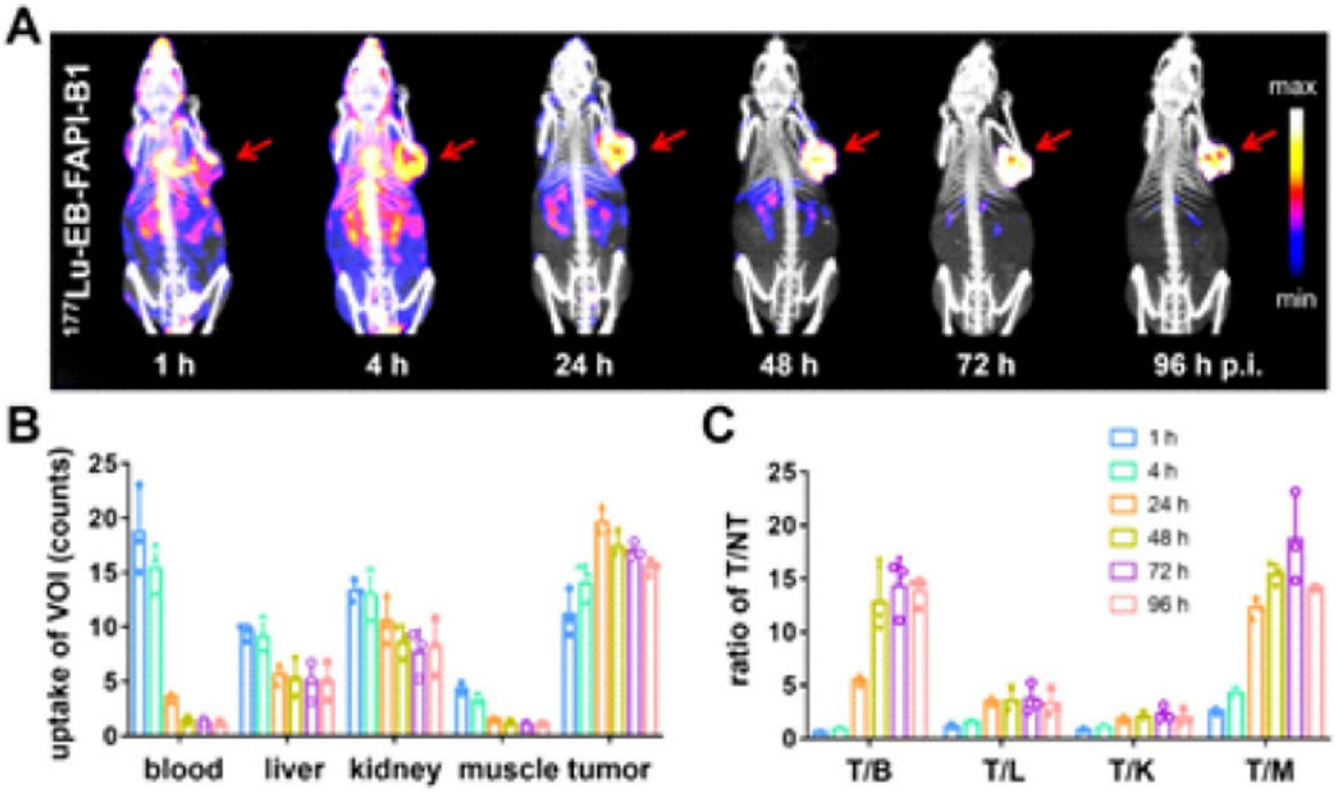

Fig. 6.

(A) SPECT/CT images in U87MG tumor bearing mice with ^{177}Lu-EB-FAPI-B1 at 96, 72, 48, 24, 4 and 1 h after injection; (B) The uptake of radiotracer in tumor, kidneys, liver, blood, and muscle; (C) The target/nontarget ratios at time intervals [92].

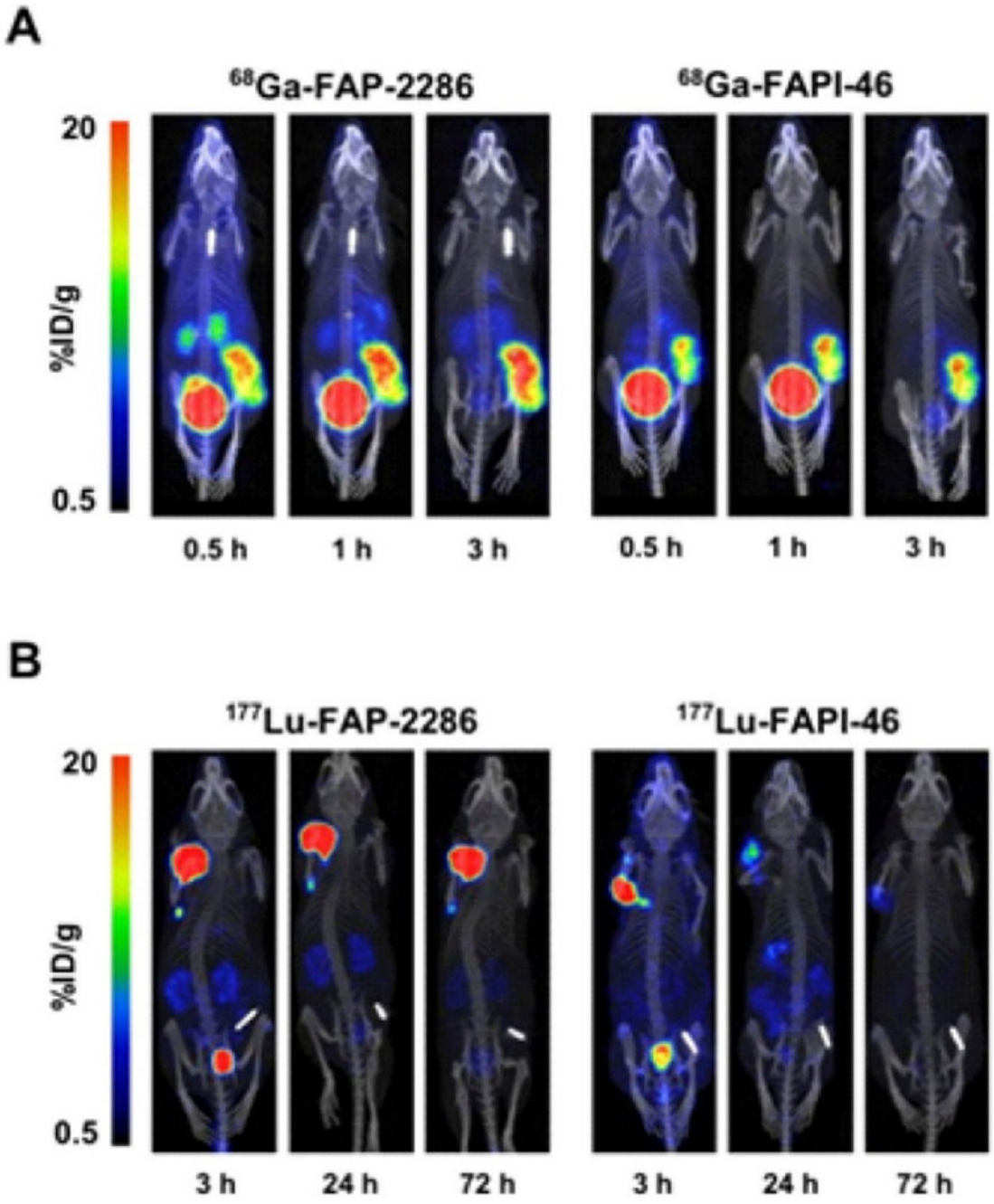

Fig. 7.

At several time points in HEK-FAP xenografts, tumor retention and biodistribution of (A) ^{68}Ga-FAP-2286 and ^{68}GaFAPI-46 (B) ^{177}Lu-FAP-2286 and^{177}Lu-FAPI-46. Adapted from ref. [97].

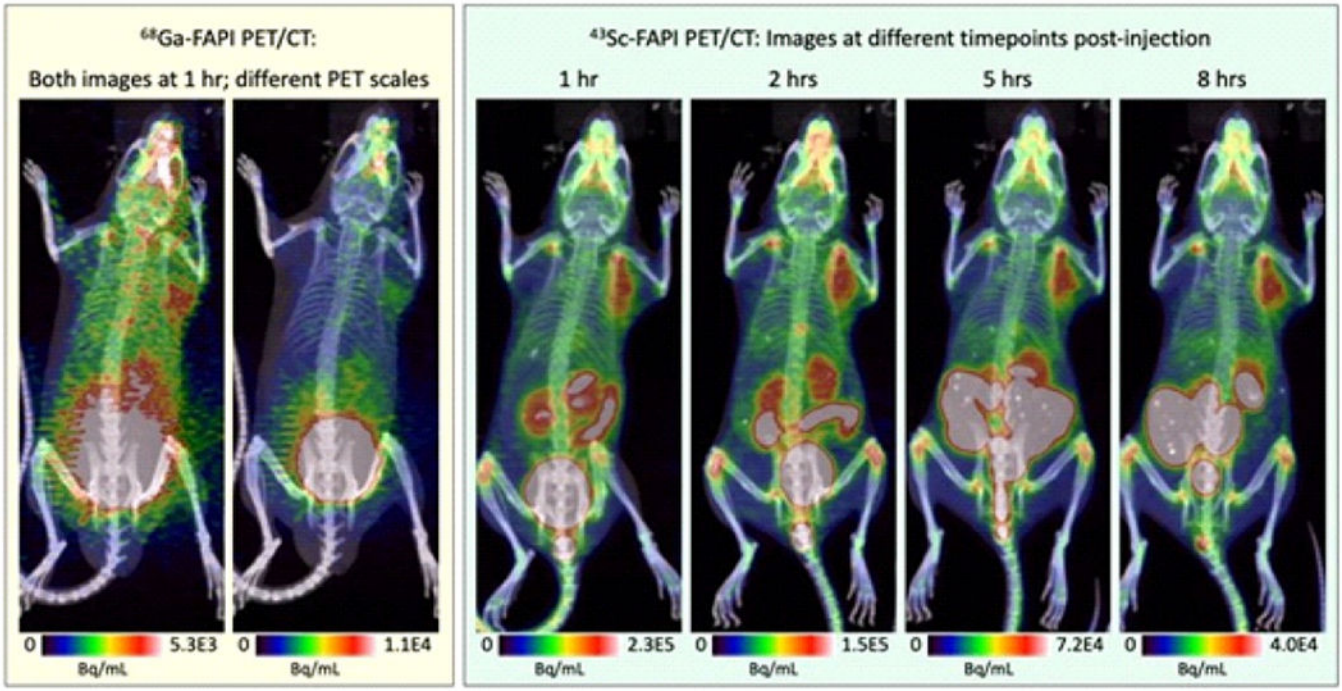

Fig. 8.

PET/CT images of ^{68}Ga-FAPI and ^{43}Sc-FAPI at several time points. Adapted from ref. [110].

Table 1

Near-infrared fluorescent tracer for targeting FAP.

Tracer	Imaging modality	Clinical trial/*in vitro*/ *in vivo* experiment	Key finding	Reference
DY-676-COOH DY-676-maleimide	NIRF * Imaging	*In vitro* evaluation of human melanoma and fibrosarcoma cells *In vivo* experiment on mice xenograft models of human fibrosarcoma and melanoma	FAP expression levels in different xenograft models correlated with local tumor fluorescence intensities	[29]
^{64}Cu-NOTA-heterodimer–ZW800 *	PET/NIRF imaging	*In vivo* experiment in mice bearing PANC-1 and BxPC-3 tumor xenografts	In contrast to single-targeted homodimers, heterodimeric imaging agents with dual radioactivity can enhance overall tumor accumulation, resulting in improved cancer imaging.	[30]
IRdye 800CW-NHS	NIRF Fluorescence Imaging	*In vitro* evaluation in six types of human cancer cells: lung squamous cell carcinoma (NCIH226), prostate (PC3, glioblastoma (U87)), colorectal carcinoma (HCT116), NSCLC (NCIH2228), and melanoma (SKMEL24) *In vivo* experiment using U87 cells positive for FAP and PC3 cells negative for FAP	By using $QCPO_1$ ***, tumors expressing FAP could be specifically imaged *in vivo*	[31]
DY-676-COOH	NIRF Imaging	*In vitro* evaluation in human Melanoma cells (MDA-MB435S), mouse macrophage cell (J774A), Fibrosarcoma cells (HT1080), and its FAP-transfected counterparts (e.g., HT1080-mFAP and HT1080-hFAP), *In vivo* experiment on xenograft mouse models	A high level of accumulation of FAP-targeting immunoliposomes in metastases and their subsequent localization in liver kupffer cells, as well as their suitable excretion in feces, substantiate their effectiveness as intraoperative contrast agents.	[32]
DY-676-COOH		*In vitro* evaluation in melanoma and breast cancer cells (MDA-MB435S and SKBR3, respectively) *In vivo* experiments on mice bearing SKBR3 and MCF-7 double subcutaneous xenografts	As evidenced by fluorescent imaging, the cargo was delivered to the nuclei of target cancer cells and stromal fibroblasts within the tumor.	[33]
DY-676-COOH		*In vitro* evaluation in murine endoglin cells and human fibrosarcoma cells *In vivo* experiments on mice organs	Macroscopic imaging using NIRF revealed distinct biodistribution patterns of immunoliposomes after injection at different times.	[34]
DY-676-COOH		*In vitro* evaluation in tumor cells (human fibrosarcoma cells, human breast, carcinoma cells, murine melanoma cells) *In vivo* experiments on mice with xenografted human cancer models	In addition to strong fluorescence quenching and activatability, bispecific liposomes were also found to selectively target cells. Their dye was targeted specifically to tumor vessels and tumor-associated fibroblasts, enabling fluorescence imaging of tumors	[35]
DY-676-COOH		*In vitro* evaluation in human breast carcinoma and human melanoma cells *In vivo* experiments in xenograft mouse models	In whole-body NIRF imaging, tumor fluorescence remained for 32–48 h after injection. Tumors, metastases, and tumor margins can be delineated intraoperatively with liposomes, as well as delivered nuclear therapeutics guided by imaging.	[36]
FL-L1-FITC FL-L1-S0456		*In vitro* evaluation in HEK293-hFAP cells *In vivo* experiment on head and neck cancer, breast cancer, colorectal cancer, and cervical cancer in mice	Injecting NIRF dye into the bloodstream can be detected the presence of malignant lesions	[37]

* Near-Infrared Fluorescence Imaging (NIRF);

** zwitterionic fluorophore ZW800–1;

*** (4-quinolinyl)-glycyl-2-cyanopyrrolidine-based small molecule for imaging of FAP.

Table 2

FAPI therapy.

Tracer	Imaging modality	Clinical trial/*in vitro/ in vivo* experiment	Key finding	Ref
[^{177}Lu]Lu-EB-FAPI-B1	SPECT/CT	*In vitro* experiment on U87MG cell *In vivo* experiment on U87MG tumor-bearing mice	It was found to be highly effective in suppressing tumor growth in U87MG tumor-bearing mice and caused negligible side effects.	[92]
[^{177}Lu]Lu-TEFAPI-06 [^{177}Lu]Lu-TEFAPI-07		*In vivo* experiment on mice bearing pancreatic cancer PDX	A remarkable inhibition of PDX tumor growth occurred with both ^{177}Lu-TEFAPI-06 and ^{177}Lu-TEFAPI-07 after accumulation in tumors that were highly FAP-selective.	[57]
[^{177}Lu]Lu-FAPI-46 [^{177}Lu]Lu-FAPI-46-F1D [^{177}Lu]Lu-FAPI-46-Ibu [^{177}Lu] Lu-FAPI-46-EB [^{177}Lu]Lu-FAP-2286		*In vitro experiment on cell lines with low (HT-1080.hFAP) and high (HEK-293.hFAP) humanFAP expression In vivo* experiment on HT-1080.hFAP and HEK-293. hFAP xenografts	In addition to tumor radiation dose (tumor uptake and residence), the peptide also offers benefits in tumor-to-background ratios. Compared to FAPI monomers, dimerization of FAPI small molecules and the cyclic peptide enhance tumor radiation dose. Albumin binders' therapeutic outcomes are closely related to their choice of albumin-binding moiety.	[107]
[^{177}Lu]Lu-DOTA-EB-FAPI	SPECT	*In vivo* experiment in U87MG and HepG2-FAP xenograft models	Different doses of ^{177}Lu-DOTA-EB-FAPI significantly inhibited tumor growth and improved tumor accumulation and retention.	[93]
[^{177}Lu]Lu-FAPI-C12 [^{177}Lu]Lu-FAPI-C16		*In vivo* experiments on mouse tumor models	In comparison to [^{177}Lu] Lu-FAPI-C12, [^{177}Lu] Lu-FAPI-C16 exhibited a greater tumor uptake	[94]
[^{177}Lu]Lu-LuFL[a]		*In vitro experiment on HT-1080 and HT-1080-FAP* *In vivo experiment in HT-1080-FAP and HT-1080 tumor-bearing mouse*	A number of promising properties were demonstrated by [^{177}Lu] Lu-LuFL, including better cellular uptake, higher FAP binding affinity, and enhanced tumor uptake as compared to FAPI-04.	[108]
[^{177}Lu]Lu-DOTA-2P $(FAPI)_2$	SPECT/CT	*In vivo* experiments on xenografts derived from patients with FAP-positive hepatocellular carcinoma and HT-1080-FAP cells	A superior inhibition of tumor growth occurred with [^{177}Lu] Lu-DOTA-2P (FAPI)2 without causing systemic toxicity	[95]
[^{177}Lu]Lu-DOTA.SA.FAPi [^{177}Lu]Lu-DOTAGA.$(SA.FAPi)_2$		A clinical trial evaluating 10 patients with various cancers	In contrast to [^{177}Lu]Lu-DOTAGA.$(SA.FAPi)_2$ and [^{177}Lu]Lu-DOTA.SA.FAPi showed significantly higher tumor uptake.	[96]
[^{177}Lu]Lu-FAP-2286		*In vitro* experiment in HEK-FAP cells *In vivo* experiment in HEK-FAP xenografts	FAP-2286 exhibits high levels of tumor cell accumulation, potent and selective FAP binding, and compelling properties related to targeted agents.	[97]
^{131}I-FAPI-02 ^{131}I-FAPI-04		*In vitro* experiment with U87MG and MCF-7 cells *In vivo* in U87MG xenograft mice	A greater degree of intracellular absorption and prolonged retention time was observed with ^{131}I-FAPI-04 than with ^{131}I-FAPI-02.	[98]
^{90}Y-FAPI-04		A clinical trial evaluating one patient with metastatic breast cancer	Pain medication was significantly reduced with this treatment, with no side effects observed, especially regarding hepatotoxicity.	[101]
^{125}I-FAPI-01 [^{177}Lu]Lu-FAPI-02	–	*In vivo* experiment using BxPC3, Capan-2, and MCF-7 cancer cells.	Cells absorbed and retained [^{177}Lu]Lu-FAPI-02 more efficiently than [^{125}I] I-FAPI-01.	[100]
[^{18}F]AlF-ND-bisFAPI [^{177}Lu]Lu-ND-bisFAPI	PET/CT	*In vivo* experiment on tumor-bearing mice with A549-FAP or U87MG	Compared to [^{18}F] AlF-FAPI-42 and [^{177}Lu] Lu-FAPI-04, the novel bivalent FAP ligand showed greater tumor uptake and retention.	[102]
^{89}Zr-AMS002-1-Fc rAb [^{177}Lu]Lu-AMS002-1-Fc rAb	PET/CT SPECT/CT	*In vivo* experiment on mice bearing HT1080 tumors	^{89}Zr/^{177}Lu-AMS002-1-Fc showed high tumor uptake as well as the ability to inhibit tumor growth without significant weight loss.	[103]
^{225}Ac-FAPI-04	-	*In vivo* experiments on xenografted mice with human pancreatic cancer	In pancreatic cancer xenograft mice, ^{225}Ac-FAPI-04 considerably repressed tumor growing.	[104]

Tracer	Imaging modality	Clinical trial/*in vitro/ in vivo* experiment	Key finding	Ref
[^{177}Lu]Lu-FAPI-46 ^{225}Ac-FAPI-46	–	*In vivo* experiments on xenografted human pancreatic cancer mice	In comparison with [^{225}Ac] FAPI-46, [^{177}Lu] FAPI-46 produced relatively slow, but longer-lasting treatment effects.	[43]
^{211}At-FAPI-04	–	*In vitro* experiment on U87MG cell *In vivo* experiment on U87MG xenografts	There was no obvious toxicity to normal organs after treatment with ^{211}At-FAPI-04, which repressed tumor growing and longer median survival in cancer patients	[102]
^{211}At-FAPI 1, 2, 3, 4,5 ^{131}I-FAPI 1, 5	-	*In vitro experiment on HEK293 and A549 cell lines In vivo experiment on PANC-1 xenograft mice*	Simple PEG-linker compounds (FAPI1) demonstrated the most promising performance in terms of cellular uptake, nuclide labeling efficiency, and *in vivo* pharmacokinetics. Moreover, PEG length did not affect uptake.	[109]

[a] LuFL: FAP targeting ligand comprising organosilicon-based fluoride acceptor (SiFA) and DOTAGA chelator.

Table 3

Ongoing clinical trials for targeting various cancers with radiolabeled FAPIs.

NCT Number	Radiolabeled	Conditions	Phase
NCT05617742	^{68}Ga-FAPI-46	Lung Cancer	II
NCT05262855	^{68}Ga-FAPI-46	Pancreatic Ductal Adenocarcinoma (PDAC)	II
NCT05641896	[^{18}F]FAPI-74	Gastrointestinal Cancers Cholangiocarcinoma Hepatocellular carcinoma, Pancreatic cancer Colorectal cancer	II
NCT05275699	^{68}Ga-FAPI	Keloid	II
NCT05898854	^{68}Ga-FAPi-46	Gastric Cancer Gastro Esophageal Junctional Cancer	II
NCT04023240	^{68}Ga-FAPI	Cancer	II
NCT05160051	^{68}Ga-FAPI-46	Tumor, Solid	II
NCT05903807	^{68}Ga-FAPi-46	Ovarian Cancer	II
NCT05410821	^{177}Lu-DOTA-EB-FAPI1 ^{177}Lu-DOTA-EB-FAPI 2 ^{177}Lu-DOTA-EB-FAPI 3	Refractory Thyroid Gland Carcinoma Refractory Thyroid Gland Papillary Carcinoma Refractory Thyroid Gland Follicular Carcinoma Refractory Thyroid Gland Hurthle Cell	II
NCT04502303	^{18}F-FDG and ^{68}Ga-FAPI	Crohn's disease	II
NCT05518903	^{68}Ga FAPi-46	Localized Pancreatic Adenocarcinoma Resectable Pancreatic Ductal Adenocarcinoma Stage 0-IIA Pancreatic Cancer AJCC v8	II
NCT04504110	^{68}Ga-FAPI-04	Epithelial Ovarian Cancer	II
NCT05506566	^{68}Ga-FAP-CHX	Tumor	II
NCT05515783	^{68}Ga-FAP-RGD	Tumor	II